Research Square

Preprints are preliminary reports that have not undergone peer review.
They should not be considered conclusive, used to inform clinical practice,
or referenced by the media as validated information.

Dietary supplementation of a Lactobacillus postbiotic modulates acute stress responses and impacts temporal variation in the gut microbiome of dogs

Erik Eckhardt

erik.eckhardt@dsm-firmenich.com

DSM (France)

Sergio Andreu-Sánchez

DSM (Netherlands)

Donato Cereghetti

DSM (Switzerland)

Balint Tamasi

DSM (Switzerland)

Anne-Sophie Boucard

DSM (France)

Gary Landsberg

Cancog Inc.

Stephanie Kelly

Cancog Inc.

Alessio Milanese

DSM (Netherlands)

Brian Klein

DSM (United States)

Elena Pagani

DSM (Switzerland)

Marco van den Berg

DSM (Netherlands)

Research Article

Keywords:

Posted Date: June 26th, 2026

DOI: https://doi.org/10.21203/rs.3.rs-10040780/v1

License: This work is licensed under a Creative Commons Attribution 4.0 International License.
Read Full License

Additional Declarations: Competing interest reported. At the time the study was conducted, E.E., S. A-S., D.C., B.T., A-S.B., A.M., B.K., E.P., and M.A.B. were employees of DSM-Firmenich AG, who provided 100% of the funding of the study.

Dietary supplementation of a Lactobacillus postbiotic modulates acute stress responses and impacts temporal variation in the gut microbiome of dogs

Erik Eckhardt[1*†], Sergio Andreu-Sánchez[2*], Donato Cereghetti[3*], Balint Tamasi[4], Anne-Sophie Boucard[1], Gary Landsberg[6], Stephanie Kelly[6], Alessio Milanese[4], Brian Klein[5], Elena Pagani[4], Marco van den Berg[2]

[1]dsm-firmenich, Houdan SAS, Houdan, France; [2]dsm-firmenich, Biotech Campus, Delft, The Netherlands; [3]dsm-firmenich AG, Geneva, Switzerland; [4]dsm-firmenich AG, Kaiseraugst, Switzerland; [5]dsm-firmenich, Biotechnology Dept., Lexington, MA, USA; [6] CanCog Inc., P.O. Box 248, Fergus, Ontario, N1M 2W8, Canada

*These authors contributed equally.

[†]Correspondence to E.E.: erik.eckhardt@dsm-firmenich.com.

Abstract

OBJECTIVES: Stress and anxiety are common in dogs but may be alleviated through dietary interventions targeting the gut–brain axis. This study investigated whether supplementation with a *Lactobacillus* postbiotic (LB fermentate HF; "LBHF"), previously shown to reduce stress in mice, could attenuate stress responses in dogs.

METHODS: Twenty-four Beagle dogs, selected for pronounced cortisol reactivity to experimentally induced stress, were randomized to receive LBHF or placebo tablets daily for 28 days while consuming a standard kibble diet. Stress challenges included 3-minute simulated thunderstorm noise test at baseline and day 28, followed by 10-minute road travel stress test the next day. Primary endpoints were plasma cortisol, with heart rate (HR) response as a secondary endpoint. Additional secondary endpoints included changes in fecal microbial communities and metabolomic composition in feces and plasma. After the final challenge, all dogs were transitioned to canned food for one week to induce microbiome shifts.

RESULTS: Whereas LBHF supplementation only tended to decrease cortisol responses during the thunderstorm noise challenge, it significantly reduced HR reactivity during this challenge, with an average HR reactivity reduction of ~20.6 beats per minute compared to placebo (P=0.021). Microbiome analysis revealed significant LBHF temporal effects, reflected in reduced intragroup variation and greater temporal stability. Concomitantly, pen-level fecal scores improved over time with LBHF. Metabolomic analyses identified an increase in circulating concentrations of tryptophan and other amino acids in plasma of LBHF-treated dogs. Multi-omic integration of fecal metagenomics and metabolomics revealed a strong correlation with HR reactivity.

CONCLUSIONS: These findings suggest that LBHF supplementation can attenuate physiological stress responses, modulate gut microbiota, and impact concentrations of multiple metabolites in healthy dogs, supporting a role for postbiotics in stress management via the gut–brain axis.

PRACTICAL APPLICATIONS: Dietary supplementation with the *Lactobacillus* postbiotic offers a natural means of reducing stress and anxiety in dogs.

Introduction

Companion and support dogs are integral members of many households. However, continuous urbanization and humanization has led to an increasing number of anxiety-related behaviors in dogs, with fear of noise ranking as highest stressors [1]. Furthermore, stress-related effects on the pet's welfare, as well as the behavioral signs arising from fear and anxiety, can be distressing, frustrating, and burdensome for owners. These behaviors may also damage property or pose a risk of injury to people or other animals. Consequently, there is a need for both behavioral and non-behavioral interventions aimed at preventing or alleviating stress in pets[2]. Remedies include pharmaceutical treatments, such as anti-depressants or alpha-adrenergic receptor blockers [3,4]. While generally efficacious, such treatments come with limitations in use and side effects, and pet owners may prefer more natural, long-term, nutritional solutions.

A growing body of evidence suggests that mood and behavior can be affected by the intestinal microbiome [5], which also seems to hold true for dogs [6,7]. Dysbiosis, an imbalance in the gut microbial composition, has been linked to various pathological conditions, including anxiety disorders [8]. Dietary interventions with ingredients such as polyphenols, protein hydrolysates and omega-3 fatty acids revealed the potential of gut microbial metabolites such as short chain fatty acids (SCFA), gamma-aminobutyric acid (GABA) and 4-ethylphenyl (4EP) acting as signaling molecules across the gut-brain axis mediating animal stress responses [9–15]. These can act locally, in the gut, or systemically [16], or by causing low-grade inflammation, for example through production of innate immune receptor ligands such as endotoxins or peptidoglycans [17,18]. One possible dietary approach consists of formulating diets that are easily digestible and thus provide less substrate for production of harmful metabolites by the gut microbiome in the hindgut [19,20]. Another approach consists of feeding supplements that promote the growth of beneficial microorganisms, such as pre-, pro-, and postbiotics. Some clinical studies have revealed putative benefits of prebiotics, defined as non-digestible nutrients for selective promotion of the growth of beneficial microbes, for wellbeing in humans [10,12], mice [21] and dogs [9]. Reports on effects in dogs of probiotics, defined as live organisms that confer a health benefit on the host, remain scarce [22]. Postbiotics, recently defined as inanimate microorganisms or fragments thereof that confer a health benefit to the host [23], are a relatively new concept. These products are more stable than their live probiotic counterparts, and hence more attractive for use in pet food. Although postbiotics are generally regarded as safe for dogs [24,25], the number of reported studies is still limited [26]. Studies with Labrador Retriever dogs reported some beneficial effects of *Saccharomyces cerevisiae* fermentate as postbiotic supplementation on physiological and behavioral responses to exercise and transport stress. Comparing low- to high-dose *S. cerevisiae* postbiotic treatment revealed variations in cytokine concentrations while having a limited effect in the gut microbiota. The postbiotic did not reduce cortisol responses following a car ride stress challenge [27]. Parallel studies suggested that postbiotic treatment upon stress induction could lead to a suppression of the innate immune system response, stability in transit time and to a higher proportion of SCFA-producing bacteria [28–30]. These findings indicate that inclusion of postbiotics in pet food can modulate immune and inflammatory parameters of healthy dogs under stress, with effects that vary by dose and formulation.

LB fermentate HF (LBHF) is a *Lactobacillus*-based postbiotic consisting of co-fermented, heat-killed proprietary strains of *Limosilactobacillus fermentum* and *Lactobacillus delbrueckii spp lactis* as well as metabolite-rich spent fermentation broth. The active component, often referred to as "*Lactobacillus* LB", has long been used for digestive health in humans [31]. Its modes of action include prevention of intestinal mucosal adhesion of pathobionts [31], strengthening of the gut barrier [32,33], bifidogenic effects *ex vivo* [34] and *in vivo* in labrador dogs [35], and stimulation of mucosal immunity in murine [36] and swine [37] models of infectious diarrhea. A recent dog study revealed a beneficial effect in digestive health and oxidative stress in labrador dogs [35].

Interestingly, a mouse study demonstrated that long-term daily feeding with LBHF-enriched diets reduced resting blood levels of corticosterone and had an anxiolytic effect on the animals under prolonged stress conditions while impacting the gut microbiome composition [38]. Plasma corticosterone/cortisol levels are regulated by the Hypothalamic-Pituitary-Adrenal (HPA) axis and correlate with cognitive impairments affecting behavior and are therefore often used as indicators of stress. Maintaining gut eubiosis will prevent release of pro-inflammatory cytokines upon stress situations, thereby not activating the HPA axis and preventing increased intestinal permeability and infections [6]. Moreover, a recent clinical trial with children with attention deficit and hyperactivity disorder (ADHD) showed that 3 months daily supplementation with LBHF significantly reduced ADHD symptoms and improved cognitive performance [39]. These observations served as rationale for the current study, in which the putative anxiolytic effect was tested using two well-known challenge models in dogs. The first model consisted of the recording of a thunderstorm, in which dogs were placed individually in an open-field room equipped with stereo speakers and subwoofer, for 9 minutes, with a 3-minute digital electronic thunder recording played back at 82 – 94 db for minutes 4 – 6 [40]. In this setting, the "fight or flight" Sympathetic-Adreno-Medullar (SAM) axis response releasing adrenaline, and/or vagally mediated autonomic regulation, may be more sensitive to treatment effect than the comparatively slower HPA axis response releasing cortisol. In this regard, heart rate (HR) reactivity is often used as an immediate, non-invasive, and continuous monitor of a SAM response [41]. Stress was thus assessed by measuring HR, blood cortisol (non-continuous), and behavioral cues. The second, milder and longer challenge, consisted of a standardized car ride in cages where the same parameters were measured. To study the mode of action, we also performed fecal metagenomic and metabolomic analyses and metabolomic analyses in blood.

Results

A two-arm LBHF intervention trial on 24 well-matched healthy dogs

A total of 24 healthy Beagle dogs successfully completed a 47-day trial (see **Fig. 1** for trial timeline). Each study arm (placebo and LBHF) contained twelve animals, cohoused in three pens of four animals each. Both study arms did not show major physiological differences at baseline (**Table 1**).

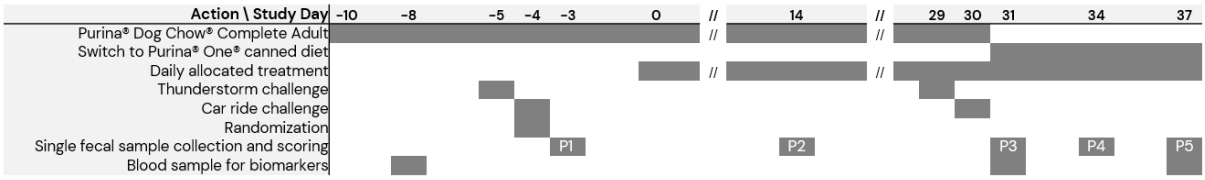


Fig. 1. Study outline. *Additional blood samples were collected before and immediately after the respective stress challenges (see text). P1-P5: fecal sampling points.*

Table 1. Baseline characteristics of treatment arms. For categorical variables, counts (total %) are expressed, and P-value is obtained from a Chi-square test. For continuous variables, mean ± standard deviation of the variable is depicted; P-values are obtained from a t-test. ALP; Alkaline Phosphatase, cALP; corticosteroid-inducible alkaline phosphatase, HR; Heart Rate, Δ values indicate change scores (cortisol: post-challenge minus pre-challenge; HR: stress exposure phase minus pre-challenge phase).

Variable	Placebo (N=12)	LBHF (N=12)	P-value
Age (years)	5.87 ± 2.61	5.5 ± 2.61	0.734
Females (%)	7 (58.3%)	6 (50%)	1.000
ALP (U/L)	57.67 ± 32.44	53 ± 26.86	0.705
cALP (U/L)	5.08 ± 0.29	6.25 ± 2.42	0.124
cALP (% of total ALP)	11 ± 4.45	13.83 ± 5.87	0.198
Δ Cortisol car	181.33 ± 79.67	178.83 ± 61.55	0.932
Δ Cortisol thunder	169.67 ± 54.36	175.33 ± 40.83	0.776
Δ HR thunder	30.94 ± 38.12	31.66 ± 23.3	0.957
Δ HR rate car	27.39 ± 39.03	4.61 ± 35.57	0.216

LBHF reduced heart-rate reactivity during the thunderstorm challenge

To evaluate the possible anxiolytic effect of LHBF, both study arms underwent two stress challenges, a thunderstorm simulation and a car ride test. These tests were conducted twice: once during the pre-treatment phase (days -5 and -4), to explore group differences and as a baseline assessment (**Table 1**), and once post-treatment (days 29 and 30), to understand the effect of LBHF supplementation (**Fig. 1**).

First, as a preliminary step, we verified that both stress tests elicited the expected autonomic response by combining pre- and post-treatment data from both groups. During the thunderstorm simulation, HR increased from 148.90 ± 33.03 beats per minute (bpm) in the pre-thunder phase to 176.89 ± 33.82 bpm in the thunder phase, decreasing to 128.17 ± 29.90 bpm in the post-thunder phase (**Fig. 2A, B**). A similar pattern was observed in the car ride test, with HR rising from 108.06 ± 22.83 bpm in the pre-ride phase to 128.84 ± 35.45 bpm during the car ride (**Fig. 3A, B**). As confirmed by generalized least squares (GLS) models, dogs showed increased HR from baseline to the stress phase in both tests, with mean HR reactivity estimated at 30.12 ± 4.05 bpm in the thunderstorm test ($t = 7.44$, $p < 0.001$) and 21.70 ± 5.99 bpm in the car-ride test ($t = 3.62$, $p < 0.001$), indicating that both tasks elicited the intended stress response.

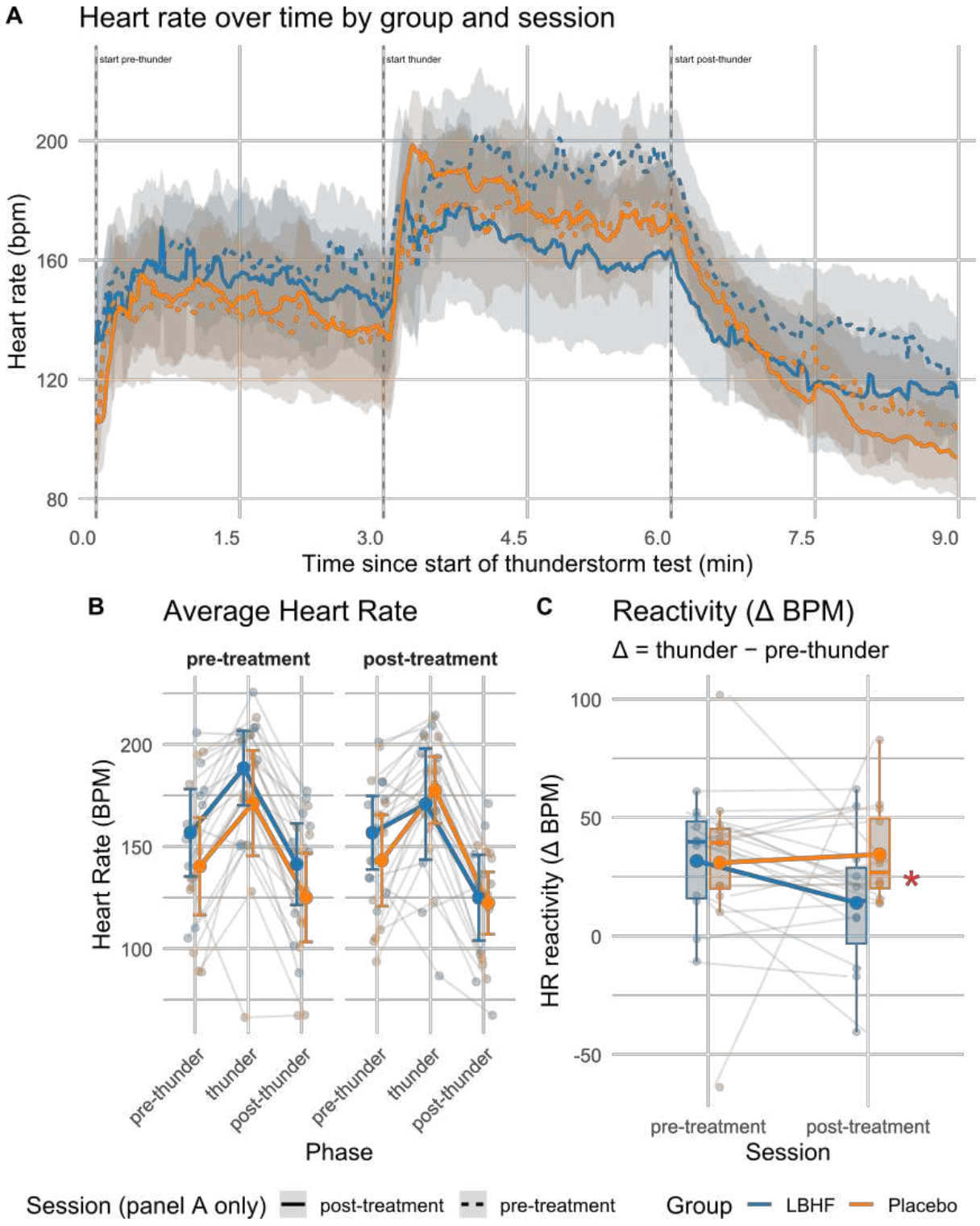


Fig. 2. Heart rate (HR) dynamics during the thunderstorm test for the two groups (LBHF, placebo) and two test sessions (pre-treatment, post-treatment). **A.** Time course of HR rate (bpm) across the 9-min test in placebo and LBHF groups, shown for pre-treatment and post-treatment sessions. Shaded ribbons indicate 95% confidence intervals. Vertical dashed lines indicate onset of the pre-thunder, thunder, and post-thunder phases, each during 3 minutes. **B.** Data aggregation into mean HR values for each phase. Thick lines with error bars indicate group means ± 95% confidence interval; thin lines represent individual dogs. **C.** Group differences in HR reactivity pre- and post-treatment. Boxes range from the first to the third quartile; horizontal bars are medians, and whiskers indicate 1.5 interquartile range. Thick lines with error bars indicate group means; thin lines represent individual dogs. The asterisk indicates statistically significant differences between LBHF and placebo (p=0.021).

Next, we assessed whether LBHF was able to reduce HR reactivity during these tasks using generalized additive models (GAMs). After 4 weeks, dogs in the LBHF group showed a significant reduction of HR reactivity by 20.56 ± 7.92 bpm in compared with dogs in the placebo group (t = -2.60, p = 0.021; **Fig. 2C**), after adjusting for sex, pen membership, and pre-treatment HR levels. In contrast, no significant post-treatment group difference in HR reactivity was observed in the car ride test (8.62 ± 14.14 bpm, t = 0.61, p = 0.552; **Fig. 3C**).

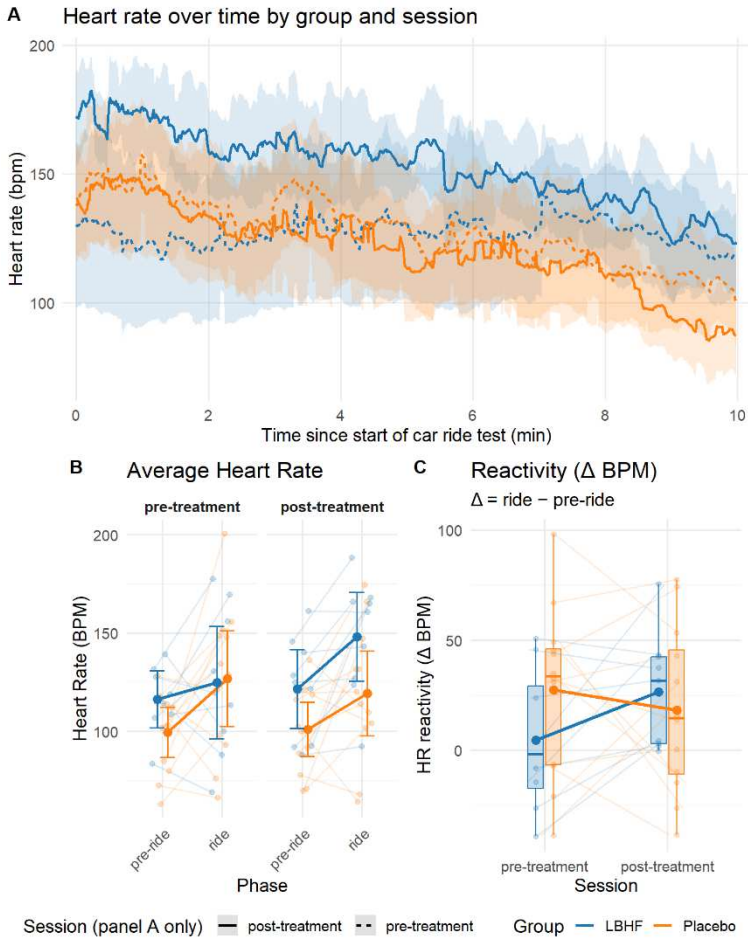


Fig. 3. Heart rate (HR) dynamics during the car ride test for the two groups (LBHF, placebo) and two test sessions (pre-treatment, post-treatment). A. Time course of mean HR (bpm) across the 10-min car ride in placebo and LBHF groups, shown for pre-treatment and post-treatment sessions. Shaded ribbons indicate 95% confidence intervals. **B.** Data aggregation into a single mean HR value for the whole car ride phase. Thick lines with error bars indicate group means ± 95% confidence interval; thin lines represent individual dogs. **C.** Group differences in HR reactivity pre- and post-treatment. Boxes range from the first to the third quartile; horizontal bars are medians, and whiskers indicate 1.5 interquartile range. Thick lines with error bars indicate group means; thin lines represent individual dogs.

In addition to HR, we investigated whether the apparent anxiolytic effect of LBHF was reflected in cortisol measurements. To assess this, we compared pre- and post-challenge differences in serum cortisol levels between the two treatment arms (**Fig. 4**). Overall, we found weak evidence for a reduction in cortisol reactivity in LHBF treated dogs in the thunderstorm test (-16.43 ± 11.81, p = 0.18). The car ride test revealed no significant differences between arms (3.36 ± 13.36, p = 0.8).

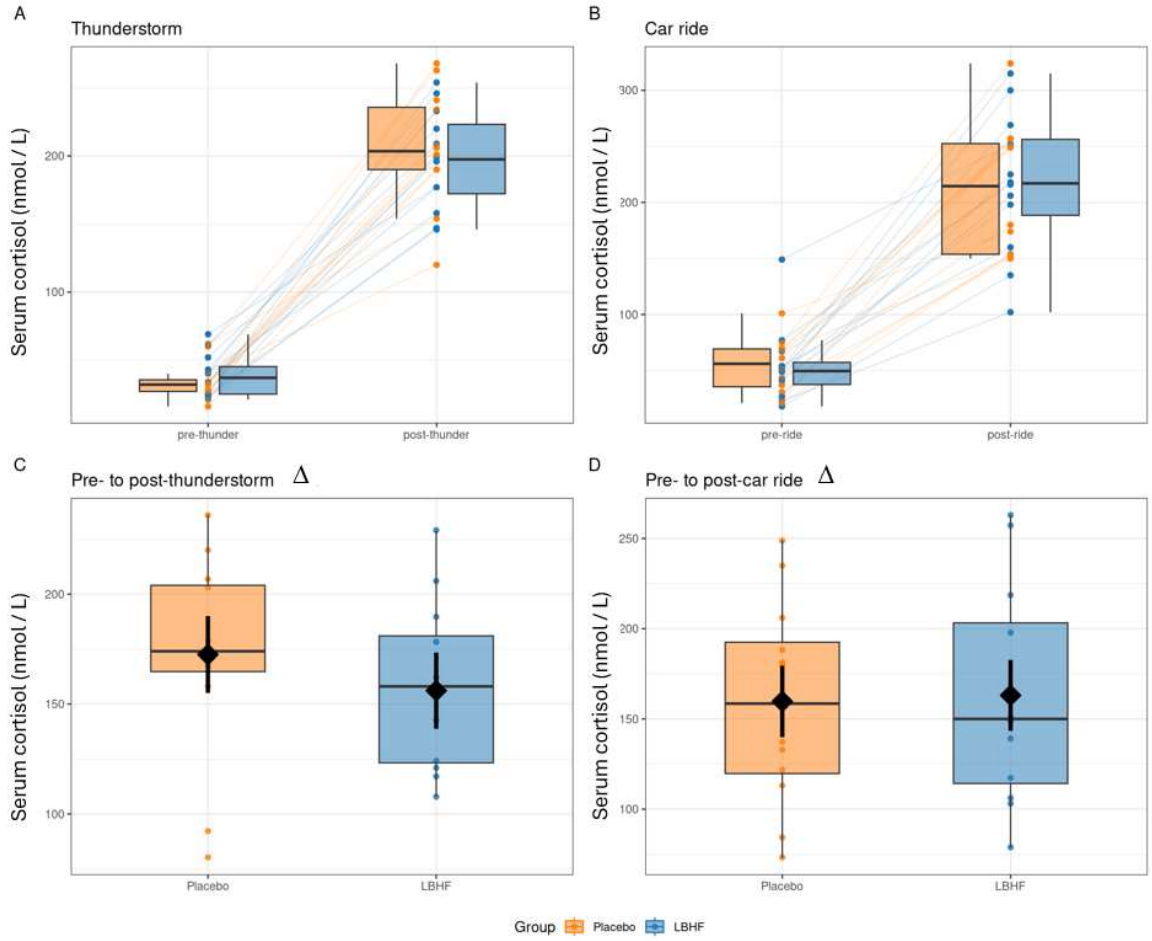


Fig. 4. Serum cortisol before and after thunderstorm (A) and car ride challenges (B). Placebo and LBHF treatment pre-minus post-challenge deltas from the thunderstorm (C) and car ride challenges (D) with their model-based estimated marginal means and the corresponding 95% confidence intervals (shown with black diamonds and thick segments, respectively).

LBHF did not affect behavioral measures

Next, we explored whether LBHF treatment could impact animal behavior during the intervention. We found no evidence of between-group differences in behavioral stress scores during the car ride challenge (log-odds ratio higher anxiety scores LHBF vs Placebo, 0.25 ± 0.84, p = 0.77). Similarly, no evidence was found for between-group differences in behavioral stress scores at any phase of the thunderstorm challenge: The respective log-odds ratios of LBHF vs control group comparisons were 1.56 ± 1.72, -0.5 ± 1.56 and -0.53 ± 1.62 (with p = 0.37, 0.75 and 0.75, respectively) for the pre-challenge, during thunderstorm challenge, and during the post-challenge phases, respectively.

Interestingly, while behavior was not significantly associated with treatment, we identified a positive association between ranked behavioral stress scores and HR during the stress phases of both the thunderstorm (linear model, effect = 0.85 ± 0.35, p = 0.019; **Supplementary Fig. 1A**) and car ride (effect = 1.42 ± 0.36, p < 0.001; **Supplementary Fig. 1B**) tests. Thus, in both tests, HR reflected behavioral manifestations of stress, supporting its validity as a physiological marker of acute stress responses.

LBHF treatment improves transit time on animal pens

We used fecal Bristol Stool Scale (BSS) as a proxy for transit time[42] for the dogs in the study. Individual fecal BSS scores were assessed at five points **(Fig. 1**). The treatment arm comparison provided evidence for lower individual BSS scores in the LBHF group after the wash-in phase (measured between days 13-16), with a log odds ratio of -2.79 ± 0.99 (p_{adj} = 0.02; **Supplementary Fig. 2**). We did not find significant differences between the two treatment groups at the remaining three post-treatment follow-up times.

We then explored whether there was an effect at the pen-level. Pen-level fecal BSS scores (lowest BSS score per pen) were recorded twice daily in the three pens of each of the two treatment arms (**Fig. 5**). The analysis of the pen-level data revealed weak evidence for lower BSS scores in the treatment arm during the wash-in phase with a log-odds ratio of -1.67 ± 0.73 (p = 0.07). The differences (expressed on the log-odds scale) between the two treatment groups were -1.33 ± 0.67 (p = 0.13) and -1.71 ± 0.95 (p = 0.2) during the treatment and anxiety test phases of the trial, respectively. However, we observed significantly lower fecal BSS scores during the diet challenge, with a log-odds ratio estimate of -1.83 ± 0.72 (p = 0.03). This suggests longer transit times in the study arm receiving LHBF, resulting in firmer stools, indicating a better response to major dietary changes.

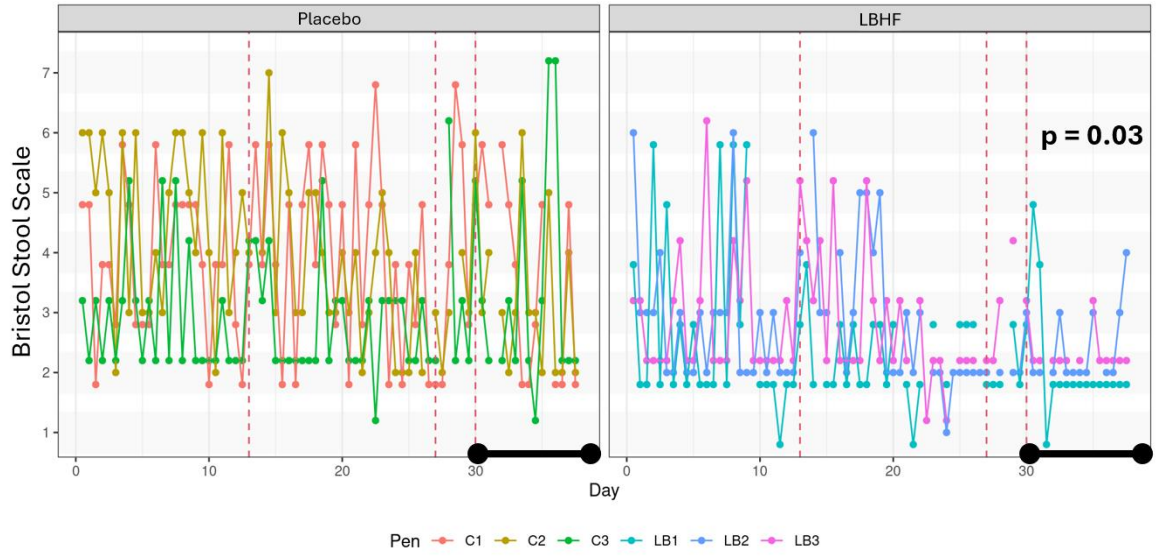


Fig. 5. **Pen-level Bristol Stool Scale scores in the two treatment arms**. The subjects of the study were kept in six pens (3 placebo and 3 LBHF). Fecal samples were collected twice a day from each pen. The dashed lines separate the four phases of the study (wash-in, treatment, anxiety test, diet challenge). The scoring scale ranged from 1 (hard lumps, consistent with constipation) to 7 (liquid stool). The switch of diet from solid to canned food is indicated by the black halter bars. During this dietary challenge, LBHF significantly improved BSS compared to placebo (P = 0.03).

Stress responses of plasma metabolites were modulated by LBHF

To further understand the physiological effects of stress and LBHF treatment, a semi-targeted metabolomic profiling of 551 plasma metabolites was conducted at two phases of the study: during pre-treatment (days -5 to 0) and during post-treatment on standard diet, prior to diet change (days 27 to 30). At each phase, measurements before and after the thunderstorm stress challenge were taken for all 24 dogs. When assessing the main sources of interindividual metabolomic variation, we identified a major impact of the dog (R^2=46%),

followed by study phase (differences between pre- or post-treatment; R^2=14.38%), pen membership (R^2=13%), analytical sample plate (R^2=3.1%), pre- or post- challenge (R^2= 2.6%), and treatment (R^2= 2%) (**Fig. 6A**). The large impact of the study phase was apparent in the first two principal components of metabolomics (**Fig. 6B**).

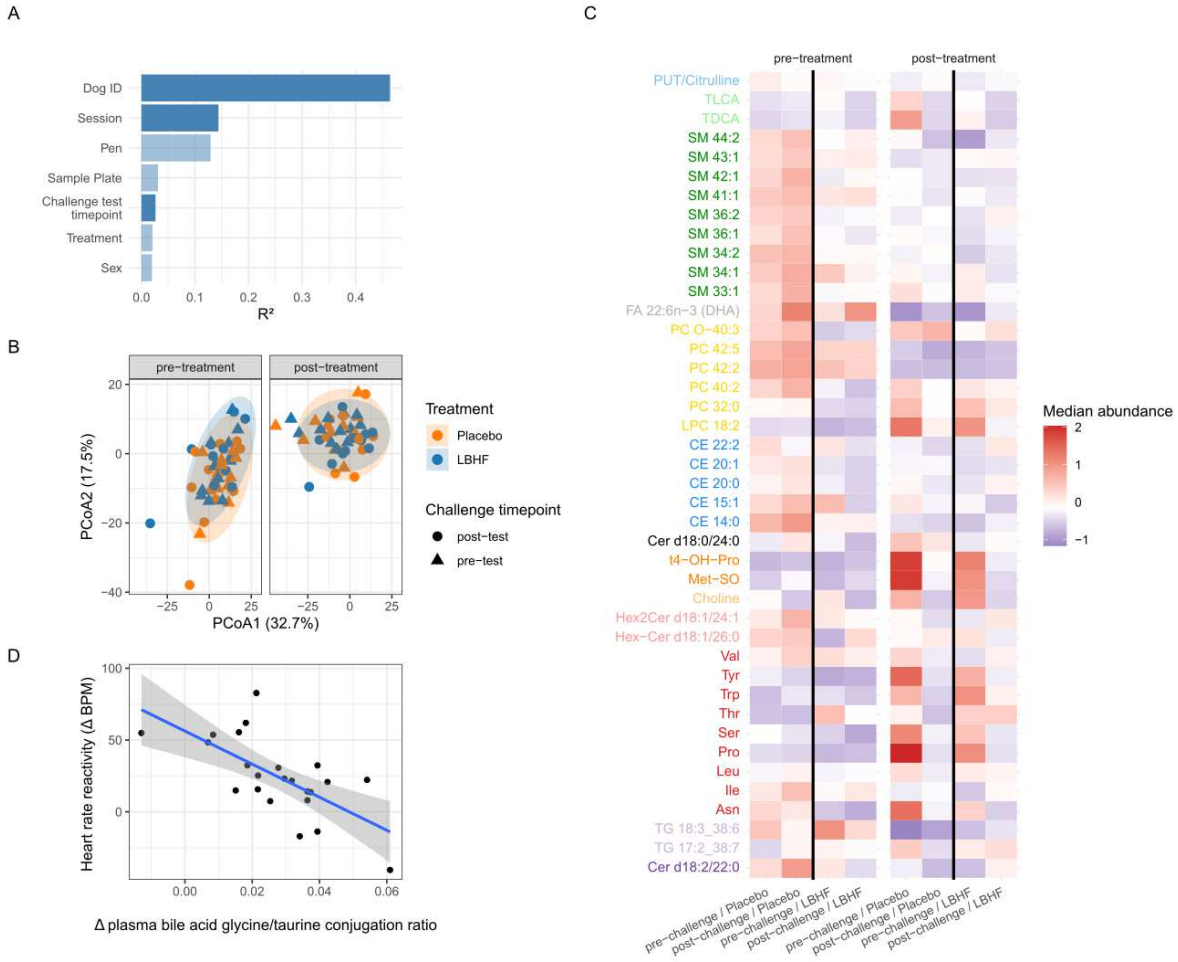


***Fig. 6. Plasma metabolome is impacted by study phase, stress and treatment**. A. Partitioning of the inter-sample variability of plasma metabolites using PERMANOVA on Euclidean distances using abundance z-scores. Bars indicate the variability explained in univariable models. B. Principal coordinate analysis (PCoA on Euclidean distances of metabolite z-scores) shows study session differences across the first and second axes of variation. C. Heatmap representing median of the z-scores of metabolites significantly influenced by LBHF-treatment in different groups and timepoints. D. Correlation between the thunderstorm HR reactivity score at the intervention phase (days 27-30) and the changes in the ratio of glycine- and taurine-conjugated bile acids between post- and pre-stress in the same timepoint.*

We performed univariate analyses to identify which metabolites, or ratios of metabolites, were impacted by stress. At baseline we found 44 metabolites (including ratios of metabolites) which significantly changed with stress (FDR<0.05, Wilcoxon rank-sum test; **Supplementary Table 2)**. The data confirmed the large increase in cortisol levels (log fold change, LFC = 2.3, p = 1.19×10^{-7}), but also cystine (LFC = 0.73, p = 1.67×10^{-6}), one of the main oxidation (stress) response indicators in plasma, and the citrulline to ornithine ratio (LFC = 0.24, p = 2.47×10^{-5}), two intermediates of the urea cycle. Rising citrulline (LFC = 0.1, p = 0.03) levels indicate NO production, which is known to increase vasodilation and improve blood flow [43,44], hence potentially relieving

stress. Interestingly, we observed that GABA ratios, including (glutamic acid + glutamine)/GABA (LFC = 0.68, $p = 3.02 \times 10^{-5}$), GABA/creatinine (LFC = -0.635, $p = 3.66 \times 10^{-5}$), GABA/glutamine (LFC = -0.686, $p = 1.75 \times 10^{-4}$), and GABA/glutamate (LFC = -0.376, $p = 8.46 \times 10^{-4}$), showed a larger fold change and lower p-values than GABA by itself (LFC = -0.640, $p = 2.70 \times 10^{-3}$), indicating the value of considering GABA in combination with other metabolites for stress assessment.

After the intervention phase, we identified stronger associations between metabolite concentrations and stress response: 278 metabolites and ratios were significantly altered by stress (FDR < 0.05, **Supplementary Table 2**). Among the top increased metabolites in plasma, we identified several free fatty acids (C14:0, C20:1, C18:1). In total, from the 9 tested fatty acids, 8 were significantly increased during stress (FDR < 0.05), corroborating earlier reports on fatty acid release upon stress in dogs [45] and in mice upon sympathetic activation of adipocyte lipolysis ultimately leading to behavioral changes [46]. Cortisol was again increased (LFC = 2.72, $p = 1.19 \times 10^{-7}$), but cystine was no longer (LFC = -0.15, p = 0.1). From the 20 measured amino acids, most were significantly lower in plasma upon stress (14 reduced, while lysine and glutamine increased, FDR < 0.05).

We assessed the effect of LBHF in metabolic concentrations in plasma before the stress challenge. Overall, we did not identify evidence for any significant metabolite changes by LBHF before stress (FDR>0.3; **Supplementary Table 3**). The largest change was seen for an increase in TG 17:2_36:4 (Wilcoxon rank-sign test, $p = 6.56 \times 10^{-4}$). Next, we assessed whether LBHF treatment could modulate stress responses at the metabolite level. For that, we built a model testing the interaction between time and treatment in the stress response (reactivity) per metabolite, assessed as the delta of the concentrations (linear mixed model). We identified 42 metabolites whose stress responses were significantly influenced by LBHF treatment (**Fig. 6C, Supplementary Table 4**). All but two showed positive associations, indicating a larger increase or a lower decrease in the metabolite abundance during stress in LBHF treatment compared with the placebo group. The largest LBHF-related effects included amino acids, such as tyrosine, valine and asparagine, and five (out of 18 tested) cholesteryl esters, among which CE 20.0 ($p = 1.59 \times 10^{-7}$), 22:2 ($p = 4.82 \times 10^{-6}$) and 20.1 ($p = 6.88 \times 10^{-6}$). In particular, the observed decrease in amino-acid concentrations in stress was less prevalent in the LBHF group for all amino acids (9 of which had significant interaction effects). Interestingly, we also observed a positive LBHF effect on circulating omega-3 (FA 22:6n-3 or DHA) (**Fig. 6C**).

Tryptophan is an important metabolite involved in three distinct pathways: kynurenine, indole, and serotonin pathways; all of which have an impact on host neural physiology. At baseline none of the measured tryptophan-derived metabolites (or metabolite ratios) were significantly affected by the stress test, while during the treatment phase most of the measured metabolites showed significant changes at stress. This included a reduction in circulating tryptophan, 3-IAA and kynurenine, but a significant increase in serotonin. Both the ratios of serotonin/tryptophan and serotonin/kynurenine also increased, indicating that tryptophan metabolism was shifted from the kynurenine and indole pathways towards the serotonin pathway. Although LBHF treatment had no significant influence on these ratios, it did lead to overall increase in circulating tryptophan.

Next, we explored the relationship between metabolic changes at stress and HR reactivity to identify possible modulators of the observed stress response. A strong correlation between stress-driven changes in the ratio of glycine-conjugated to taurine-conjugated bile acids and thunderstorm challenge HR reactivity was seen during the post-treatment phase (rho = -0.67, $p = 4.6x10^{-4}$, FDR = 0.23) (**Fig. 6D**). This suggests that greater stimulation of the bile acid receptor TGR5 (stronger with taurine-conjugated bile acids) is associated with a reduced HR response to stress, as was for example shown in rats [47]. This correlation was, however, not present during the pre-treatment season (rho = -0.04, p = 0.8, FDR = 0.99). This bile acid ratio was not impacted by LBHF treatment during the post-treatment session (Wilcoxon rank-sum test, p = 0.67), and thus, it is unlikely to explain the observed calming effects of the LBHF supplementation.

We also assessed whether one-month supplementation with LBHF affected plasma levels of alkaline phosphatase (ALP), notably its steroid-inducible form (corticosteroid-inducible ALP; cALP), a marker of stress in dogs. We did not observe and effect of LBHF on either marker (**Supplementary Fig. 3**)

LBHF intervention promotes fecal microbial community stability

Next, we set out to uncover the impact of LBHF on gut microbial communities. Fecal material was collected at five timepoints (P1 – P5 in **Fig. 1**) and shotgun sequenced (samples of two dogs lacked for the last time point). Major sources of variability in species-level microbial communities were identified by performing a PERMANOVA analysis on Aitchison inter-sample distances (**Supplementary Fig. 4A**). Univariable tests identified significant effects for several study variables ($p<0.05$). These included: donor variation (R^2 = 31%), time (P5 is end of diet [R^2 = 10%], P4 is diet change [R^2 = 3.6%], P3 is stress challenge [R^2=2.9%], P2 is treatment study [R^2 = 4.7%]), BSS (as a proxy for transit time, R^2=5.1%), sequencing depth (4.7%), pen membership (R^2 = 9.8%), and treatment (R^2 = 3.6%).

To further assess a possible interaction effect between treatment and time, we computed Principal Response Curves (PRC), a multivariate tool suited for time-series analysis with several interventions. We identified a significant interaction between time and treatment in the first constrained axis (permutation test, $p = 8x10^{-3}$) (**Supplementary Fig. 4C**), indicating treatment differences through time. These differences were particularly enriched for a decrease of *Bifidobacterium* species (GSEA test, NES = -1.95, FDR = $1.51x10^{-6}$), namely *B. globosum*, *B. animalis*, *B. pseudolongum*, *B. canis* and *B. pullorum* (**Supplementary Fig. 4D**).

To further visualize community similarity between treatments and time, we performed a principal coordinates analysis (PCoA) of the Aitchison distances (**Fig. 7A**). We observed a significant relationship between the two major axes of variation in the community (PCo1 and PCo2, accounting for 17.82% and 9.8% of interindividual variation respectively) and both time (linear mixed-model, P1-P5, $p_{PCo1} = 41.22x10^{-25}$, $p_{PCo2} = 3.74x10^{-5}$), and treatment (linear mixed-model, $p_{PCo2} = 0.05$). Visualization of the two first axes also suggested that the dispersion of communities in the LBHF group was lower than that in placebo group, indicating a convergent, less individual-specific community in the intervention group. This is hard to visualize due to the dominance of inter-donor variability in the first axes of variation identified by PCoA. Thus, as an additional exploratory analysis, we performed a tensor factorization of the microbial communities. This dimensionality reduction

technique enabled us to project complete time trajectories for each dog into a few axes of variability (five components, R^2 = 33.2%). A similar observation in which a lower dispersion could be found in treated samples could be seen in the first axes of variation (**Fig. 7C**), while a PERMANOVA test on the interindividual Euclidean distance based on the five first components identified a significant treatment effect (R^2 =15.3%, p = $2x10^{-3}$; this association remained significant when further axes were computed, $R^2_{20components}$ = 10%, p = $2x10^{-3}$). Among the top axes, Component 3 was significantly associated with treatment (linear model, FDR = $7.5x10^{-3}$). By looking at the top species loading this component, we observed that a different temporal trajectory between treatments could be seen after P2 (**Supplementary Fig. 4B**). These species included several *Bifidobacteria* that were significantly less abundant in the LBHF group, and other taxa including *Fusobacterium*, *Erysipelotrichaceae* or *Lactobacillus*, and a group of species that were higher in the LBHF-treated group, from genera such as *Anaerobiospirillum*, *Sutterella*, *Holdemanella*, and *Ventrimonas*. *Bifidobacteria* was also found significantly enriched for negative PRC loads, indicating a convergent signature between two different analytical approaches.

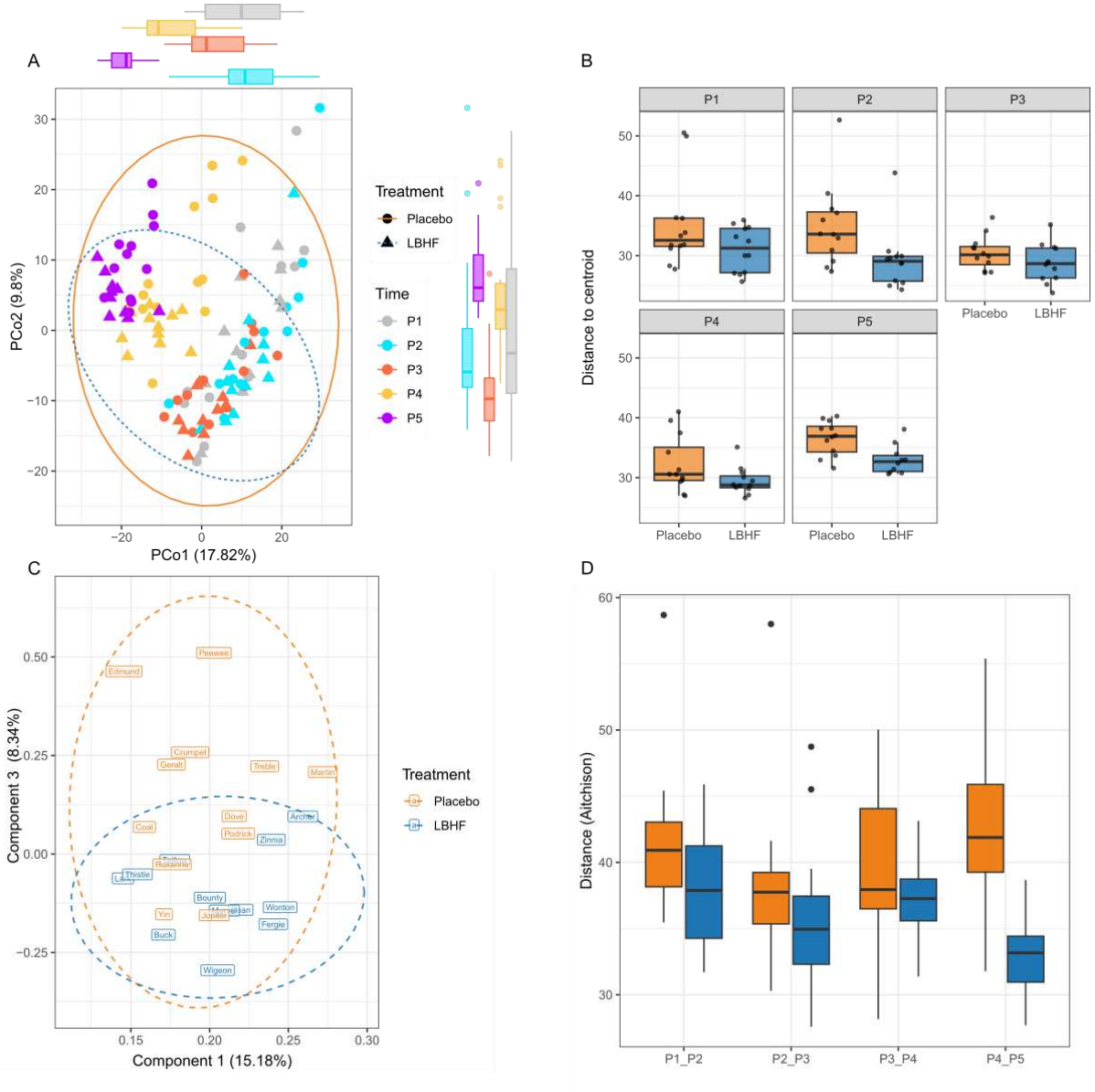


Fig. 7. Variability in the microbial community during the study is driven by time and treatment. A. PCoA of Aitchison distances displays clustering per timepoint (color), which is displayed as boxplots in the margins of the plot. Different treatments cluster differently in PCo2 and are highlighted with ellipses. **B.** Distance from centroid (beta dispersion) of each of the treatment groups through time. **C.** Tensor factorization of Aitchison distances, showing temporal trends between P1 and P4 per each of the dogs (IDs displayed in plot), showing a lower dispersion for LBHF-treated dogs. **D.** Aitchison distance between samples from the same dog at two different timepoints displays a trend for more stability in the LBHF-treated group.

Next, we set up to further explore the observed lower dispersion in treated samples. For that, we performed a beta dispersion analysis, thus computing a centroid per treatment group and assessing distances to this centroid per sample (**Fig. 7B**). This analysis uncovered a difference of dispersion between groups (permutation test, $p < 5x10^{-3}$). However, such differences could also be seen at baseline, which might indicate that this was not a feature of the intervention, but of the dogs themselves (mean difference distance to centroid baseline = 5.6, $p_{P1} = 0.057$; distance to centroid P2 = 5.6, $p_{P2} = 0.031$). Thus, we aimed to remove the variability attributed

to baseline by using the abundance of taxa with respect to baseline (deltas) as an input for the analysis. After this, differences in beta dispersion remained significant among treatment groups ($p < 0.005$). This suggests that while baseline differences exist between the groups, the treatment exacerbates such differences, as could also be inferred from an increased PRC through time in the treated group (**Supplementary Fig. 4C**).

We further investigated whether this community convergence could be related to a lower degree of change, i.e. a higher stability of the microbial community of dogs receiving LBHF in comparison to the placebo group during the trial period. For that, we compared the distances between samples from the same dogs in contiguous time points. We observed a higher stability between time points in the LBHF treatment group in comparison to placebo (linear mixed model, LBHF effect = -4.18, $p_{permutations} = 4.5x10^{-3}$) (**Fig. 7D**). This difference in microbial similarity was seen throughout the trial but was particularly large when comparing the two time points during and after the dietary intervention ($p = 5x10^{-3}$). We wondered if this community-wide feature (higher stability) could also be seen at the level of strains. At the microbiome genetic level, the same animals tended to have more similar microbial single nucleotide variant (SNV) profiles through time than non-cohoused unrelated animals (linear model, same animal effect = -0.05, $p < 2x10^{-16}$), or co-housed animals (same animal effect = -0.024, $p = 1.25x10^{-9}$). When we checked whether the higher stability at the community level also translated to lower genetic distances between strains we did not identify significant differences in the similarity between the same animals either overall (linear model, LBHF effect = -0.01, p = 0.3), or through time (likelihood ratio test (LRT), p = 0.4), although the average similarity was higher in LBHF-treated dogs (marginal genetic distance, LBHF = 0.313, placebo = 0.315), which might point to a slightly higher strain-level stability.

Overall, these results seem to indicate that LBHF treatment might have an effect on the overall dog microbial community, as supported by significant associations between treatment and principal axes of variation (PRC, PCos and tensor factorization), which was also reflected in a significantly lower intragroup variation, even after normalizing for baseline composition, and a higher temporal stability of the microbial community during the study duration, in particular, during the dietary intervention.

LBHF intervention influences microbial taxonomic abundance but not sample diversity

Given the observed effect in communities driven by both time (including stress [P3] and diet [P4, P5] challenges) and treatment, we further set up to explore the effect of treatment and time in Shannon diversity. We observed temporal increases in Shannon diversity in both treatment groups, occurring between P2 (start of the trial) and P3 (end of stress phase) (linear model, $effect_{P2\text{-}P3} = -0.24$, $P = 1.3x10^{-3}$, $FDR = 5.4x10^{-3}$), and between P3 and P4 (start of diet intervention) ($effect_{P2\text{-}P3} = -0.16$, p = 0.04, FDR = 0.07), while a trend for diversity reduction was observed between P4 and P5 (end of diet intervention) ($effect_{P4\text{-}P5} = 0.15$, p = 0.06, FDR = 0.08). No significant differences in the time effect were found between treatments, although there was a trend for a lower diversity reduction at P5 (after the diet switch) in LBHF-treated samples ($estimate_{Placebo\ P5\ effect\text{-}LBHF\ P5\ effect} = 0.12$, p = 0.4) (**Supplementary Fig. 5A**).

Next, we tested individual taxa to identify changes produced by the challenge and treatment. In total, out of 204 species tested, 129 had significant changes between consecutive time points (FDR < 0.05) (**Supplementary Fig. 5B, Supplementary Table 5**). These differences were mainly driven by changes produced by the diet challenge, including 72 taxa significantly changing abundance between P3 and P4, and 54 changes between P4 and P5. In contrast, we identified 26 changes between P1 and P2, and 23 between P2 and P3.

We then explored the overall differences between LBHF treated samples and controls and identified significant changes in five microbial species (FDR<0.05) (**Supplementary Fig. 5C-F, Supplementary Table 6**), including *Sutterella* (linear mixed effect model, units on CLR space, $effect_{LB}$=3.08, p = $8.6x10^{-4}$, FDR=0.04), *Bifidobacterium globosum* (effect=-2.46, p = $1.1x10^{-4}$, FDR=0.04) and *Fusobacterium A* (effect=-2.92, p = $8x10^{-4}$, FDR=0.04), which we previously identified in multivariate analyses to drive differences between the study arms. In addition, two poorly annotated taxa, a bin from the CALVGN01 genus (family *Erysipelotrichaceae*) and UBA9414 (family *Lachnospiraceae*) were positively associated with the LBHF group. We were, however, underpowered to test microbiome-wide interaction effects with time. Thus, we focused on these taxa associated with treatment groups (**Supplementary Table 7**). From them, the unknown novel species in the genus CALVGN01 showed the most evidence for time interactions (LRT, p = 0.04). Particularly, we observed a significantly higher increase of CALVGN01 through time (comparing P1 and P5) in LBHF (**Supplementary Fig. 5F**) (estimate=3.39, p = 0.01).

Overall, this indicates several convergent taxonomic changes throughout the study, possibly driven by situations of coinhabiting, stress, and diet challenges. The diet challenge resulted in the largest number of taxa with significant changes. LBHF-treated dogs had an overall distinct taxonomic abundance of five taxa.

Fecal metabolomic profiles are impacted during the intervention

Three of the collected fecal samples per animal, corresponding to time points P1 (baseline), P3 (end of stress phase) and P5 (end of diet-challenge phase), were used to measure fecal metabolomics, with a semi-targeted approach, yielding measurements for 558 metabolites. After removal of 303 of them, where over 80% of the samples were under the detection limit, we used 303 metabolites for subsequent analyses.

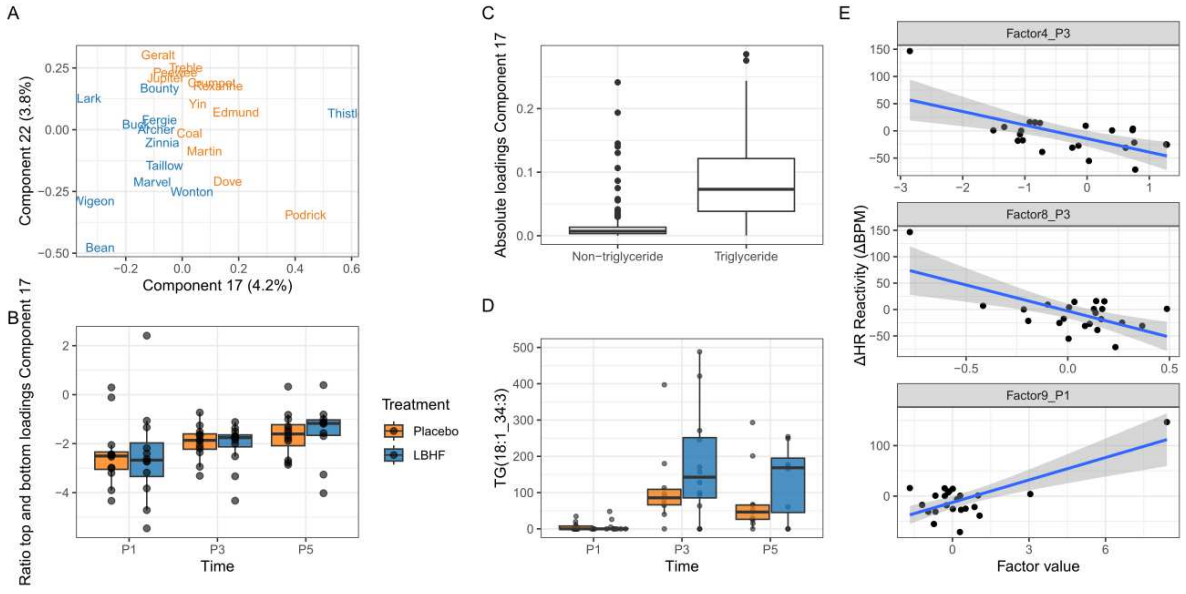


Fig. 8. LBHF-treatment effect on fecal metabolomics and co-variation with species abundance. A. Tensor factorization of untargeted fecal metabolomic profiles identifies a factor (PC17) related to LBHF treatment. Temporal trajectories per dog subject are depicted in the reduced dimensions and highlighted with the animal's name. **B.** Log ratio of top and bottom metabolites loading PC17. **C.** Comparison of the absolute loadings of glycerol metabolites vs non-glycerol metabolites for PC17. **D.** Top load of PC17 significantly associated with treatment. **E.** Association between MEFISTO factors including variation of both metabolites and microbiome, which were selected in a penalized lasso regression model with the delta (intervention phase-baseline) of thunderstorm HR reactivity scores.

We performed a tensor decomposition to obtain low dimensional factors representing longitudinal trends of the fecal metabolomic profile. Out of 24 tested components (i.e., combinations of metabolites of which temporal changes explain variability between animals), Component 17 (C17) showed a trend separating both treatments (Wilcoxon rank-sum test, $p = 2.32 \times 10^{-3}$, FDR = 0.05) (**Supplementary Table 8**) (**Fig. 8A, B**), and the overall factors showed a trend distinguishing between study groups (hypoRF test, p = 0.12; highest variable importance for C17, 4.2 standard deviations above the mean importance, assessed using the Gini index). The top loading metabolites for C17 were triglycerides, both as negative and positive loads. In fact, triglycerides were on average 1.15 standard deviations above the absolute loads of other metabolites (linear model, $p < 2 \times 10^{-16}$) (**Fig. 8C**). This seems to point to changing concentrations of triglycerides found in feces during the trial. Overall, this multivariate analysis indicates a small temporal effect of LBHF treatment in fecal metabolomics.

Then we performed univariate testing for each fecal metabolite. We identified 190 metabolites with significant concentration shifts in time (FDR < 0.05; **Supplementary Table 8**). In total, 128 metabolites changed their abundance between P1 and P3, and 123 between P3 and P5. Due to the relatively small effect of the intervention (which could only be seen at C17 in the tensor analysis), we focused on the univariate testing of the intervention effect in only the top loading metabolites for C17. The triglyceride TG(18:1_34:3) showed a significant interaction effect between time and treatment (LRT, $p = 9.8 \times 10^{-3}$, FDR = 0.05; **Fig. 8D**). This metabolite was higher at P5 in LBHF-treated samples in comparison to placebo.

Fecal metabolomic and microbiome (co)variation is linked to stress response

Next, we investigated shared variation between fecal microbiota and metabolomics data using MEFISTO, which identifies latent factors representing major axes of covariation between the two modalities. We decomposed the variation into 10 factors, explaining a total of 65% and 38.26% of variability for metabolome and microbiome respectively. Only factors 1, 3 and 7 explained over 1% of variability in both metagenomic and metabolomics views. Factor 1 and Factor 7 were strongly linked with time (study phase) (linear mixed model, Factor 1 $time_{P1-P5} = -3.49$, $p = 8.63 \times 10^{-35}$; Factor 7 $time_{P1-P3} = 1.61$, $p = 2.5 \times 10^{-6}$). None of the factors were associated with the intervention, indicating a weak effect in the covariation of microbial and metabolic composition of feces.

We then used these factors to predict treatment response, as the delta of the thunderstorm challenge's HR reactivity in pre-treatment and post-treatment seasons. Using a regularized regression model (lasso), where we repeated cross-validation to pick the optimal regularization parameter 100 times, we identified three MEFISTO factors that were often selected to predict the ΔHR reactivity (**Fig. 8E**). These were Factor 4 at P3 (selected in 41% of models, median coefficient in standard deviations = -0.11), Factor 8 at P3 (selected in 20% of models, median coefficient = -0.07) and Factor 9 at P1 (selected in 48% of models, median coefficient = 0.12). The analysis showed that dogs with higher scores on Factor 4 and Factor 8 at P3, and lower scores on Factor 9 at baseline, showed the greatest decreases in HR reactivity from pre-treatment to post-treatment. Factor 4 mainly explained variation in abundance of species (10.9% species, 0.9% fecal metabolites), and was driven by a series of unknown species, belonging to the genera *Metalachnospira*, *Gallibacter* or MGS1590. Factor 8 mainly explained fecal metabolomics variation (0% species, 6.1% metabolites), including negative loads of C14:1-OH, C16:2, 5-AV or creatinine, among others. Factor 9 mainly explained species variation (5.87% species, 0.003% metabolites), including negative loads to *Phascolartobacterium*, *Faecalibacillus intestinalis*, *Phocaicola caprophilus*, and positive to *Bifidobacterium canis* and *Bifidobacterium globosum* among others. Interestingly, our previous univariate and multivariate analyses identified that several members of the *Bifidobacterium* genera were reduced in the LBHF-treated group, while here we found that they are positively linked with an axis of variation related to an elevated ΔHR reactivity, i.e. stronger stress response in post-treatment compared to pre-treatment.

We tested whether the LBHF effect on ΔHR reactivity could potentially be mediated through microbial and metabolic features collected in these embeddings. We identified a mediation of 68.7% of the effect from Factor 9 at P1 ($p = 0.36$), 66% mediation from Factor 8 at P3 ($p = 0.3$), and the estimated mediation was 0% for Factor 4 at P3 ($p = 0.9$). While no significant effects were found ($p > 0.05$), this seems to indicate that some of the LBHF effects might be mediated through Factors 8 or 9, while it is unlikely that Factor 4 mediates LBHF-effect.

Overall, this discovery warrants further investigation to determine whether the observed reduction in HR reactivity associated with LBHF is mediated by the observed microbial or metabolomic signatures described.

Discussion

448 Under threatening situations, dogs, as other animals, activate their stress response systems: the rapid
449 sympathetic-adreno-medullar (SAM) and the slower hypothalamic-pituitary-adrenal (HPA) axis [48,49]. The
450 respective release of catecholamines and glucocorticoids is highly controlled and triggers a range of cellular,
451 physiological, and behavioral responses to endure the situation and return to normal as fast as possible.
452 However, repeated or chronic stress could lead to irreversible damage such as cardiovascular dysfunctions,
453 diabetes, depression, and lifespan reduction [50,51]. Dietary interventions may relieve some of the direct or
454 indirect effects of stress and, importantly, offer a non-pharmaceutical approach with a favorable safety profile.
455 Gut microbiota, and especially their metabolites, are more and more recognized as a critical element of
456 general health, including mental health, stress prevention, and relief, via the so-called gut-brain-axis [5,7,52].
457 Hence, long-term dietary interventions such as pre-, pro-, and postbiotics are explored to mitigate stress
458 situations and responses in humans and animals [6,49,53].

459 A human study evaluating *Lactobacillus plantarum* DR7 probiotic in stressed adults revealed reduced plasma
460 cortisol levels as well as reduced plasma pro-inflammatory cytokines [54], illustrating that microbial interventions
461 can mitigate stress-induced inflammatory responses [55]. Postbiotics offer a more stable alternative to probiotics
462 [23] and some are used for digestive health in humans [31]. A recent study showed that long term dietary
463 supplementation with a *Lactobacillus*-based postbiotic also caused a marked reduction of baseline serum
464 levels of corticosterone in mice after repeated stress challenges and altered their behavior in ways that
465 suggest a calming effect of the postbiotic [38]. These changes were associated with significant changes in the
466 fecal microbiome of the animals, suggesting that the postbiotic acted via the gut-brain axis. The present study
467 attempted to replicate these findings in dogs by using two well-controlled stress tests, namely, a simulated
468 thunderstorm and a car-ride challenge.

469 In contrast to the mouse study, the present study with dogs did not reveal an effect of longer term postbiotic
470 supplementation on baseline levels of cortisol, the mammalian homolog of murine corticosterone. This might
471 relate to the different set-up of our dog study versus the mouse study; in the latter the baseline was
472 determined after three weeks of treatment wherein the mice underwent multiple variant stress tests. In our
473 study, however, LBHF did significantly reduce HR reactivity during the post-treatment thunderstorm challenge,
474 suggesting a cortisol-independent calming effect of the postbiotic. Of note, whereas the mouse study had
475 revealed a long-term corticosterone-reducing effect of the postbiotic, the corticosterone levels in the mice did
476 increase to the same extent in LBHF-fermented fed mice as in control mice during stress challenges [38], which
477 further suggests glucocorticoid-independent calming effects of the postbiotic in both studies, mediated via the
478 HPA-axis. Whereas cortisol can be considered a good marker of chronic stress, it is not the main driver of HR in
479 the short term, let alone HR reactivity, which is driven by catecholamines (not assayed in the present study).
480 The present study revealed some other HR reduction-corroborating observations, further indicating
481 stimulation of the SAM-axis. Plasma citrulline was increased, which is an indicator of increased NO levels (not
482 assayed in the present study) inducing vasodilation [43,44]. Secondly, the increased plasma fatty acid levels not
483 only provide for an alternative energy source during periods of stress, they are also implied to enhance the
484 distensibility of arteries [56] and are well-known for their hypotensive activity [57]. Both contribute to improved

485 blood flow, supporting the observed HR reductions and thereby relieving stress. Interestingly, whereas LBHF
486 did not significantly affect serotonin/tryptophan or serotonin/kynurenine ratios and thus did not significantly
487 affect a shift of tryptophan from the kynurenine to serotonin pathway, LBHF nevertheless led to an overall
488 increase in circulating tryptophane, suggesting a sparing effect on this essential amino acid.

489 Surprisingly, the calming effect noted during the thunderstorm challenge was not replicated in the car ride
490 challenge model. In the latter model, no effect on HR reactivity was observed. This could be due to several
491 reasons. First, the trial design may not be ideal as the car ride challenges occurred on the day after the
492 thunderstorm challenge. Both models involved preparation of the dogs in the same procedure room, and the
493 dogs may have experienced a strong degree of anticipation from the recent thunderstorm experience as they
494 were being prepared for the car ride one day later. However, this effect should be similar across subjects or
495 primarily affect those that reacted more strongly to the thunderstorm (i.e., the placebo group), which is not
496 observed during the car ride, where the LBHF group appears to respond more in post-treatment car ride, albeit
497 not significant so. On the other hand, both groups had higher pre-car ride baseline cortisol levels (54 nmol/L)
498 as compared to the pre- thunderstorm (37 nmol/L) levels, which may reflect some degree of anticipatory
499 stress when the dogs were prepared for the car ride. Second, during the car ride, HR reactivity was lower than
500 during the thunderstorm challenge and reached lower peak values, consistent with a somewhat less acute
501 challenge type, and potentially leaving less room for modulation by the treatment. Beagles typically show HR
502 of approximately 115 bpm during transport [58], while thunderstorm exposure has been reported to elicit HR
503 values of around 150 bpm. This suggests that the thunderstorm challenge likely presents the more acute and
504 likely more severe stress challenge, perhaps more consistent with fear[59]. The values observed in the present
505 study therefore fall within the plausible physiological range reported in literature. Third, the HR data collected
506 during the car ride was generally noisier, requiring exclusion of more animals, and showing greater variability
507 both within and between dogs in their responses. Neither model showed significant differences in behavioral
508 stress scores, although their non-parametric nature makes it more difficult to measure quantifiable differences
509 in the scores. However, although also not significant, the Bristol Stool Scale scores did show a tendency
510 towards improvement upon the post-treatment challenge (days 27-30 in Fig. 5), suggesting a positive impact
511 of the LBHF-treatment. In summary, the stress tests revealed a calming effect of the postbiotic in an acute
512 stress challenge involving loud and unpredictable noises, suggesting a benefit of the postbiotic in reducing
513 stress responses.

514 Our study further showed that supplementation with the postbiotic leads to a gradual improvement in
515 intestinal transit time, including during a transition from solid kibble type diet to liquid canned food. These
516 changes were associated with a more stable fecal microbiome composition. This observation is in line with a
517 recent five-week intervention study with Beagles using the same postbiotic, which indicated that the
518 postbiotic stabilized fecal scores and microbiome composition in challenging conditions [35]. The observation is
519 also in line with numerous clinical studies in which the active ingredient in LBHF improved fecal score and
520 transit time versus placebo in humans [31 60] or in studies with weaned pigs (*Sus scrofa*) orally challenged with
521 F18+ enterotoxigenic *E. coli* [61].

Whereas LBHF led to a stabilization of the overall fecal microbiome with apparent beneficial effects on intestinal transit time and, hypothetically, on stress responses, observed taxonomic changes are difficult to interpret. The bifidogenic effects of LBHF previously reported in human[34] and canine feces[35] were not confirmed in the current study. In fact, a small decrease in several species of *Bifidobacteria* was found. Similarly, levels of *Fusobacteria*, generally considered beneficial in dogs [62], were also slightly lower in the LBHF group. Both observations could indicate subtle changes in digestibility with less colonic availability of undigested dietary protein or undigested carbohydrates, the preferred substrates of *Fusobacteria* and *Bifidobacteria*, respectively. Interestingly, the study by Xu et al on the effect of LBHF in *E. coli*-challenged weaned pigs showed that the postbiotic had mostly affected mucosal microbial communities, specifically in the jejunal mucosa, as opposed to fecal communities [37]. Validation of such effects in dogs awaits the development of reliable non-invasive mucosal sampling technology. The study by Xu et al also demonstrated an effect of LBHF on jejunal crypt cell proliferation -an indicator of wound repair- and reduced jejunal IL-8 production, illustrating the effect of the postbiotic on the upper GI tract. A gut-barrier strengthening effect of the postbiotic, recently confirmed in a study with human colonic organoids [33] may have also occurred in the dogs in the current study, thus contributing to GI and overall health.

Taken together, the current study showed that 5-week supplementation of dogs with the postbiotic LBHF stabilized the gut microbiome and reduced acute stress responses in dogs subject to thunderstorm simulations. The anxiolytic effects were related to subtle changes in the fecal metabolome and in amino-acid sparing effects in blood during stress responses. Lastly, the stabilizing effects on the gut microbiome may have contributed to significant improvement in transit time upon a diet switch, thus confirming previously reported benefits across species.

Materials and Methods

Animal Husbandry

All procedures were reviewed and approved according to the principles of The Animal for Research Act of Ontario and the Canadian Council on Animal Care (CCAC). The study was conducted at the facilities of Transpharmation Canada Ltd. Clinical trial number: not applicable.

Twenty-six Beagle dogs (3.4 to 10.6 years old, sex balanced) were screened for inclusion in a 47-day placebo-controlled, investigator blinded parallel group intervention trial in three phases (baseline phase, stress phase, and diet challenge phase, Figure 1). During the baseline phase (Days –10 to –1), the basal diet (Purina® Dog Chow® Complete Adult) was washed-in gradually. At day -8, dogs were examined by a veterinary and blood was collected for clinical chemistry, alkaline phosphatase (ALP) measurements – including corticosterone inducible ALP -, and biomarker analyses.

The pre-treatment assessment included a thunderstorm test (Day –5) and a car ride test (Day –4) which served to obtain baseline values and to randomize animals to their respective treatment groups. For this, following baseline anxiety assessments, one dog was excluded from the study due to a lack of cortisol reactivity, along

with one dog that exhibited poor appetite on the basal diet. The 24 remaining dogs were ranked according to their individual cumulative post-stress serum cortisol levels and subsequently allocated to one of two treatment groups (LBHF or placebo) using an ABBAABBA block pattern according to descending cumulative rank. Animals in each group were subsequently co-housed in three pens of four animals each for the duration of the study. Prior to pen housing, a baseline fecal sample was taken on day -3 for metagenomic and metabolomic analyses.

During the entire trial, food consumption, general health observations (twice daily), and fecal scoring using the Bristol Stool Scale (BSS) [42] at the pen level were assessed daily (in case of multiple fecal samples per pen, the most loose stool was scored). From day 0 on, all animals in each group received their respective investigational product. The *Lactobacillus* postbiotic ("LBHF") or placebo (microcrystalline cellulose (MCC)) were administered in custom prepared treats (Synergie Prod SAS, Sevremoine, France) consisting of tablets with dicalcium phosphate, pig liver extract as palatant and colorant, silicic acid, and magnesium stearate to which LBHF or MCC were added. Test substance and placebo were visually indistinguishable, and their containers were coded to ensure blinding. During the intervention phase, each dog received 300 mg LBHF or 300 mg MCC, during the afternoon feed.

Post-treatment thunderstorm and car stress assessments were done on Days 29 and 30, respectively at which time additional blood and fecal samples were taken. After the last car ride challenge, a diet challenge was performed from day 30 to 36. To this end, all dogs were abruptly switched to a canned food diet (Purina® ONE®). Fecal and blood samples were taken at the start, halfway point, and end of the challenge. Dogs received their respective test substances until day 36.

The primary endpoint consisted of the maximum cortisol response during stress tests. Secondary endpoints included HR reactivity, metagenomics (fecal) and metabolomics (fecal and blood).

Stress tests

At the start of each test session, dogs were moved from their housing pen to an adjacent procedure room. Here, a chest-strap heart rate monitor (Polar H10, Polar Electro Oy, Kempele, Finland) was applied. Similar Polar® chest-strap devices have previously been validated for accurate heart-rate measurement in dogs [63], supporting the suitability of this method for canine HR recording. The strap was positioned just behind the forelimbs with the sensor placed on the left side of the chest, over a small area that had been shaved at least one day prior. Contact gel was applied to improve electrode-skin conductance. Once the strap was in place, dogs were acclimated for at least 2 minutes before a 3-minute baseline HR was recorded at rest. The dogs were then either transferred to the thunderstorm testing arena or placed in the travel crate, which was secured in the vehicle for the car-ride test.

HR was continuously recorded during the challenges at 1 Hz (events per second) and subsequently aggregated into 1-minute averages for analysis. Since data was transmitted from the sensor via Bluetooth, brief connectivity interruptions occasionally occurred during recording. As irregular movement can impact connectivity, this is more common during car rides, due to motion of the vehicle (acceleration, braking, uneven roads) and the dog

repositioning or stabilizing itself in the travel cage [64]. Accordingly, any 1-minute periods with insufficient valid data to compute a reliable HR average were excluded from the dataset. As an additional preprocessing step, any 1-minute HR value below 55 bpm was excluded as physiologically implausible. In a few cases, prolonged signal loss prevented reliable HR estimation across the entire test session, resulting in the exclusion of data from four dogs, one from the thunderstorm test and three from the car-ride test.

Thunderstorm test

The procedure was adapted from previously published studies [65,66]. Each dog was tested individually in a dedicated arena (approximately 2.9 × 3.3 m) equipped with three cameras for video monitoring. Each session lasted nine minutes and comprised three phases: a 3-minute pre-thunder (baseline) phase, during which dogs could freely explore the arena; a 3-minute thunder exposure phase, involving playback of a thunderstorm track delivered through a stereo system a peak sound level of 104 dB; and a 3-minute post-thunder (recovery) phase, conducted in silence.

Behavioral responses were assessed separately for each test phase (pre-thunder, thunder, post-thunder) using three approaches: (I) automated activity tracking, (II) manually coded activities, and (III) observer-based anxiety ratings. Locomotor activity was quantified automatically from video recordings using EthoVision® XT (Noldus, Leesburg, VA), which detected the dogs' movement path in meters based on camera-tracked position data. Within the same software, additional behaviors were manually recorded by a trained behavioral analyst via keypress, including inactivity duration (time spent sitting or lying, and not engaging in any other behaviors) and head-movement frequency during inactive periods. Anxiety-related behaviors were assessed from the video recordings using a rating scale derived from established indicators of noise-related fear and anxiety in dogs [11,66]. Two dimensions were rated: intensity, defined as the severity of anxious behaviors (1 = none, 6 = severe), and duration, defined as the proportion of time anxious behaviors occurred (1 = none, 6 = most of the time). The evaluation considered both active (characterized by increased locomotor activity including startle, bolting, vigilance, scanning, aimless pacing or circling, digging, scratching or climbing walls, active retreat, and vocalization), and passive or inhibited manifestations of anxiety (reflecting behavioral inhibition and reduced activity, such as panting, lip-licking, shaking, yawning, salivating, cowering, tail-tucking, freezing near walls, vigilance, and inactivity). A behavioral stress score was then calculated for each test phase by averaging the intensity and duration ratings. Dogs were tested at approximately the same time of day for each assessment (±30 minutes). Before each session, the room was cleaned to prevent odors from affecting test performance.

Car ride test

The test was conducted in a cargo van, with the dog placed inside a wire-mesh crate (60.96 × 76.2 cm) secured in the rear compartment. The crate had wire-mesh sides and a plastic floor covered with a rubber mat to provide traction. Three cameras mounted within the vehicle recorded behavior from the front, back, and side views. Two technicians were present: one drove the vehicle, while the other monitored the dog for behavioral assessment. Each ride lasted 10 minutes, and sessions were standardized as much as possible to minimize inter-animal and inter-session variability. That is, the driver maintained a steady speed, and environmental factors such as noise and temperature were controlled.

Behavioral responses were monitored both in real time by the passenger technician and retrospectively from video recordings. Real time observations included vomiting, urination, defecation, and vocalization. The first three behaviors were scored as present or absent, while vocalizations were quantified in 2.5-minute intervals and subsequently converted into a 0–3 frequency score, as outlined in **Supplementary Table 1**. Video footage from the three cameras mounted within the van was analyzed by a trained behavioral analyst. The analysis assessed changes in body position (i.e., frequency and duration of standing, sitting, and lying down) and anxiety-associated behaviors, including lip licking, panting, salivating/drooling, escape attempts/frustration, restlessness/repetitive movement, and yawning/mouth gaping; all recorded via keypress in EventMark software (Transpharmation Canada Ltd.). The number of events for each behavior was counted within each 2.5-minute interval, and these counts were subsequently converted into scores (0–3 for most behaviors; 0–4 for lip licking), as per Table 1. A behavioral stress score was then calculated for the entire 10-minute car ride by summing all scores across the four 2.5-minute intervals, with a maximum possible score of 88. Dogs were tested at approximately the same time of day for each assessment (±40 minutes). Before each session, the crate and mat were cleaned to eliminate residual odors that could affect test performance.

Biological Sampling

Whole blood for serum cortisol analysis (Antech Diagnostics, Mississauga, Ontario) was collected a minimum of 2 hours before thunderstorm and car ride challenges, and 8 minutes after the thunder simulation and 8 minutes after the car ride. Additional blood samples were taken for biomarker analyses twice during the study. All serum and plasma samples were frozen at -80°C until shipped for analysis. Fecal sampling was performed at 5 timepoints: once during baseline (P1), once during the treatment phase (P2), once at the end of the anxiety phase (P3), and twice during the diet challenge phase (P4 and P5). Animals were monitored constantly over a period of 3 days to ensure naturally voided samples were collected within approximately 15 minutes of voiding. The animals were placed in metabolic housing as necessary to enable fecal collections. Metabolic housing occurred following anxiety testing to avoid interfering with the results. If a sample was not produced, animals were housed individually overnight, and naturally voided fecal samples were collected first thing in the morning. Overnight samples were only used for analysis if a fresh voided sample could not be collected within the 3-day monitoring period. Fecal samples were photographed and scaled. Samples were taken from the center of each voided sample and subdivided into three aliquots. All collected samples were stored in barcoded collection tubes with preservation fluid (OmniMET and OmniGene from DNAGenotek North America) for metabolites and microbial DNA, respectively, until laboratory analyses.

DNA extraction, library preparation and sequencing

DNA was isolated using the QIAGEN DNeasy PowerSoil Pro Kit, according to the manufacturer's instructions (Qiagen). Isolated DNA was quantified using a Qubit Flex fluorometer and the Qubit™ dsDNA HS Assay Kit (Thermofisher Scientific). DNA libraries were prepared using the Watchmaker DNA Library Prep Kit (7K0019-1K). Genomic DNA was fragmented using a master mix of Watchmaker Frag/AT Buffer and Frag/AT Enzyme Mix. IDT xGen UDI Primers and IDT Stubby Adapters were added to each sample followed by 7 cycles of PCR to construct the DNA libraries. The final DNA libraries were purified using CleanNGS magnetic beads (CleanNA)

and eluted in nuclease-free water. Following elution, the libraries were quantified using the Qubit™ fluorometer dsDNA HS Assay Kit. Libraries were circularized and sequenced on the Element AVITI platform using the 2x150 Cloudbreak FreeStyle sequencing kit.

Metabolomics measurements

Plasma and fecal metabolites were quantified using a targeted metabolomics approach based on the Biocrates MxP® Quant 500 kit (Biocrates Life Sciences AG, Innsbruck, Austria), and 630 metabolites from 26 compound classes were profiled. Samples were processed according to the manufacturer's instructions. Analysis of sample extracts as well as of reference standards and quality controls was carried out by UHPLC and flow injection analysis, both coupled to tandem mass spectrometry. An Agilent 1290 series UHPLC system coupled to a 6500 + QTrap mass spectrometer equipped with an Ion-Drive Turbo V® ESI source (both Sciex, Foster City, CA, USA) was used for the analysis. Chromatographic and mass spectrometric parameters were set as indicated by the manufacturer of the kit. Data analysis was carried out on the Biocrates WebIDQ software.

Genomic processing

Creation of a dog genomic database

For metagenomic analysis, it is necessary to have a collection of genomes from the species present in the samples. Here, we used 2,669 bacterial genomes from PATRIC [67] and supplemented them with 7,081 metagenomic assembled genomes (MAGs) from dog metagenomes [68] previously generated[69] [70].

From these 9,750 genomes, we applied filtering thresholds of ≥75% completeness and ≤5% contamination based on CheckM estimates [71]; 79.33% of the genomes passed this filter. We then dereplicated the genomes using dRep (v3.5.0) [69] at 99.5% average nucleotide identity (ANI) with a minimum of 50% overlap, resulting in 3,134 representative genomes.

These genomes were annotated taxonomically using GTDB-Tk (v2.3.2; database version r214) [72]. All genomes had at least a family-level annotation, and for genomes missing lower-level annotations, the highest previously assigned taxonomic level was used as a placeholder.

A Kraken2 database was constructed using the dereplicated genomes and the dog reference genome (GCF_011100685.1_UU_Cfam_GSD_1.0) [73]. Low complexity genomic regions were masked using DustMasker [74].

Taxonomic classification

To estimate species-level taxonomic abundances, reads from the FASTQ files were classified against the genomes identified in the previous step. Reads were filtered using Fastp (v0.20.1) [75], discarding reads shorter than 15 bp, with more than 5 ambiguous bases, with over 40% of nucleotides with a Phred below Q15, or that had sequence complexity below 30%. Taxonomic classification was performed running Kraken2 (v2.07), with a filter for a minimum of 0.1 confidence, and taxa abundances were obtained with Bracken (v3.0)[76] with a minimum of 50 counts per taxa required for abundance estimation.

Normalized taxonomic tables were generated by center-log transforming (CLR) the abundances, with the addition of a pseudocount of 1. In specific analyses, a baseline normalization was also done in CLR-transformed data by subtracting each taxa per sample by their abundance at the baseline timepoint, this is thereafter referred to as baseline-normalized tables.

Statistical Data analysis

Stress endpoints

Heart rate data

Individual minute-level HR data were aggregated within the relevant phases of each test (*pre-thunder*, *thunder*, and *post-thunder* for the thunderstorm test; *pre-ride*, and *ride* for the car-ride test), yielding one mean HR value per phase and session (pre- and post-treatment). HR reactivity was then calculated for each dog and session as the difference in mean HR between the stress exposure phase and its preceding HR baseline phase, a widely used approach in stress-response research [77]. In the thunderstorm test, this corresponded to the change in HR from the *pre-thunder* (3-min) to the *thunder* (3-min) phase, whereas in the car-ride test it represented the change from the *pre-ride* (3-min) to the *ride* (10-min) phase.

As an initial manipulation check, we assessed whether the stress tasks elicited the expected physiological response using generalized least squares (GLS) models. These models tested whether the mean HR reactivity exceeded zero, reflecting an average increase in HR from baseline to stress phase, while assuming equal correlation between repeated measures within each dog (compound symmetry) and allowing residual variances to differ across sessions and treatment group. Treatment effects on HR reactivity were assessed using separate generalized additive models (GAMs) with Gaussian errors for the thunderstorm and car-ride tests. In both GAMs, pre-treatment baseline and stress phase HR values were included as penalized smooth terms, sex as a stratification variable, and pen membership (cohousing of animals in the same treatment group) as random effects.

Cortisol analysis

To assess treatment effects on cortisol response during the thunderstorm and car-ride tests, we compared differences in serum cortisol levels before and after each challenge between the two treatment arms. Similar to the HR reactivity analysis, treatment effects were analyzed using GAMs with Gaussian errors. Group comparisons were adjusted for pre-treatment cortisol deltas (using penalized spline terms to account for nonlinear relationships), sex (as a stratification variable), and pen membership (as a random effect).

Behavioral manifestations of stress

Behavioral stress scores were calculated for each animal during both the thunderstorm and car ride challenges. For the thunderstorm challenge, scores were computed separately for each test phase (pre-thunder, thunder, and post-thunder), whereas for the car ride challenge, a single score was calculated for the entire 10-minute ride. These scores were treated as (partially) discrete ordinal responses and analyzed using proportional odds logistic regression models. The models adjusted for pre-treatment score levels during each challenge (using penalized spline terms), sex as fixed effect, and pen membership as a random effect. To

capture the correlation structure in the repeated measures model for the thunderstorm, the model also included dog-level random intercepts.

To investigate the extent to which physiological measures correspond to behavioral indicators of stress, we analyzed the association between HR and behavioral stress scores in both models. For each dog and session, HR values from the stress phase of the test (3-minute *thunder* phase; 10-minute *car ride*) were paired with the corresponding score. Linear mixed-effects models were then fitted with HR as the dependent variable and behavioral score as the predictor, including a random intercept for dog to account for repeated measures across pre- and post-treatment sessions. Because behavioral stress scores are ordinal in nature, they were rank transformed prior to analysis.

Bristol Stool Scale analysis

The individual BSS scores were compared between control and LB-treated groups with a longitudinal proportional odds logistic regression model. The model constraints the treatment-arm difference to zero for the pre-treatment measurement time (constrained longitudinal data analysis) and adjusts for sex differences as fixed effects and pen membership as random effects (both interacted with time).

We used a hierarchical generalized additive model (HGAM)[78] to model the time trajectories of the pen-level fecal scores on the log-odds scale over the course of the study. We modeled the main time trend of the evolution of the fecal scores with a thin-plate regression spline and the pen-level deviations from the main trend were captured with factor-smooth interactions with a shared penalty term. Morning and afternoon sample collection times were differentiated with a fixed effect term. We compared the two treatment arms at each of the four discrete phases of the study (wash-in: days 0-13, treatment: days 13-27, anxiety tests: days 27-30 and diet challenge: days 30-34) using a Wald test adjusting for multiplicity with a single-step, max-t type adjustment[79].

Alkaline phosphatase analysis

We used generalized additive regression models to compare the effect of the LBHF treatment on alkaline phosphatase levels and steroid-induced ALP fractions at follow-up. We assumed a log-normal and beta conditional outcome distribution for ALP and steroid-induced isoenzyme fraction, respectively. The group comparisons were adjusted for the pre-treatment baseline values (included with penalized spline terms to capture nonlinear relationships), sex (stratification variable), pen membership random effects. Asymptotic Walt tests conducted for hypothesis testing.

Microbiome data analysis

PERMANOVA analysis

Aitchison distance was used in a PERMANOVA analysis with the R package vegan v2.7-2 (adonis2). Only dogs with all timepoints available were retained (three dogs missing the final timepoint were removed), ensuring a balanced repeated-measures design. Each explanatory variable was tested in a univariate PERMANOVA model against the distance matrix. We classified variables into within-subject and between-subject sources of variation: (i) Within-subject variables, variables that change over time within the same dog (e.g., time,

sequencing depth, Bristol stool scale), were analyzed using restricted permutations within dogs. In the vegan package, this was implemented by supplying the dog ID as a strata/blocking factor, which prevents shuffling observations across individuals and correctly respects repeated-measures dependence. (ii) Between-subject variables, variables that do not vary within dogs (e.g., treatment, pen membership, sex), were analyzed using permutations at the dog (subject) level, because such effects cannot be tested by shuffling observations within. Instead, we permuted whole subjects using the plots argument of permute::how(), which allows exchangeability of whole experimental units when the effect varies between subjects

Principal Response Curves and enrichment of loads

To explore the interaction between treatment and time in a multivariate setting, we computed principal response curves[80] using the PRC function from the vegan R package on CLR-transformed species abundance data. Statistical testing was done via permutations, setting plots with dog IDs as strata (type='free') and within type='series'. Testing was done with the anova function (first = True).

Species loadings were extracted, ranked, and used in a gene set enrichment analysis (GSEA) as implemented in the R package clusterProfiler v4.8.3. We ran this analysis to test for enrichment of genera among the high and low loads of PRC.

Principal Coordinate Analysis

Aitchison distance was also used in a Principal Coordinate Analysis (PCoA). The first two principal coordinates (PCo) were tested against time and treatment, while accounting for sex and Bristol Stool Scale in a linear mixed model with a random intercept per dog ID. Overall time effect was assessed by comparing a model without and another with time using the R function 'anova'.

Beta dispersion

Beta dispersion analysis was performed using vegan's beta disper function, followed by permutest using dog IDs as blocks for the permutation. Per timepoint, differences in dispersion were tested with the R package coin, using the function oneway_test, and approximating the distribution via permutations. This analysis was repeated using baseline-normalized Aitchison distances.

Community similarity in time

Time consistency was tested by extracting Aitchison distances between samples from the same dog at two continuous timepoints. Per timepoint, we performed a one-way test comparing distances between treatment groups. An overall test was done combining all time points, for that, distance was associated with treatment and controlled per time as a fixed-effect and ID as a random intercept. P-value was estimated by performing 2,000 permutations of the label per ID (keeping the treatment within ID consistent through time) and then computing the probability of observing effect sizes from the permuted null distribution as or more extreme as the absolute value from the estimate in the non-permuted data.

Tensor factorization

Tensor factorization of complete time series was run using TEMPTED[81] v0.1.1 on CLR-transformed species abundance data. By default, the number of extracted components was set to 5. We tested the association of treatment with a Euclidean distance based on the extracted components using vegan's adonis2. This analysis was repeated at different component numbers and using baseline-normalized taxonomic profiles.

Within species genetic variation and between sample similarity

To assess similarity between samples at a subspecies level, we meta-genotyped metagenomes using GT-Pro (v1.0.1) [82], using the default '20190723_881species' database. While this database was constructed based on human microbes, we assumed that overall similarity trends could be captured even if the profiled SNVs do not cover all the diversity of dog bacteria. GT-Pro was then run with default parameters or merged paired-end reads. We selected a total of 58 species where we could identify an average of 500 SNVs in at least 50 samples. Per individual species, we used strainfacts (v0.4.0b) [82] to filter the genotypes (minimal allele frequency of 5%) and samples (minimal horizontal coverage of 15%). We randomly selected 500 SNVs and computed genetic distances between samples using sfacts 'pdist' function to generate normalized distance matrices per species.

To test the pen membership effect on this distance, we filtered out distances of samples from the same donor and kept only distances between samples from the same timepoints. A linear mixed model then was applied using genetic distance as dependent variable, and an interaction between time and 'same pen' as independent, while allowing a random intercept per species. To test for donor effect, we filtered distances in continuous timepoints and filtered distances between members of the same pen that belonged to different donors. We then fitted a linear model using distances as dependent variables, 'same animal' and time comparison as fixed-effects variables, and a random intercept for species. To test for treatment effect, we only used longitudinal distances (so not using unrelated dogs), in linear mixed models testing for treatment as the independent fixed variable, accounting per time comparison, and a random intercept per species.

Alpha diversity analyses

Species-level Shannon diversity index was computed using vegan's diversity function on relative abundances. Testing between time, treatment and indexes was done via linear-mixed models. Two models were fitted, a simple model with no interaction between treatment and time, and an interaction model. In both cases, sex and Bristol Stool Scale were used as covariates, and a random intercept per dog ID was included.

To extract time effects between different contrasts we used emmeans (v1.10.4) in the simple model. To understand the effect of treatment and its interaction with time, we used emmeans in the interaction model to extract contrasts per timepoint, and interaction effects for different time contrasts.

Univariate taxa modelling

CLR-transformed species-level abundances were fitted per species against time and treatment group, as described for alpha diversity. We focused on contrasts between contiguous timepoints (i.e. microbial changes that occur between two subsequent times). Treatment effect was assessed by checking for the interaction effect of treatment in P4 in contrast to P3. We applied the BH-FDR adjustment to address multiple testing.

Plasma metabolomics statistical analysis

Metabolite prevalence was quantified as the percentage of samples where the metabolite was detected above the detection limit. Metabolites with a prevalence below 20% were removed. We used PERMANOVA (adonis2) for partitioning the interindividual variation, using Euclidean distances of metabolites' z-scores between samples, and a similar permutation strategy as described for microbiome.

To detect metabolite changes between pre- and post- stress challenge, we ran Wilcoxon signed-rank tests. To detect treatment effects, we first computed the delta between before and after challenges per individual, at each timepoint (baseline and test). Delta values were normalized using the blom method for inverse rank normalization. Linear mixed models were fitted per metabolite, using the normalized delta values as a dependent variable, and the interaction of study phase (baseline/test) and treatment group, as independent, while accounting for the subject. We adjusted for multiplicity to control the FDR with the Benjamini-Hochberg procedure.

We tested the correlation (Pearson) between the deltas of metabolite abundances per study phase (post-stress – pre-stress) and deltas of the heart rate changes per time point (post-stress – pre-stress). We applied the BH-FDR adjustment to address multiple testing.

Fecal metabolomics statistical analysis

Metabolite prevalence was quantified as the percentage of samples where the metabolite was detected above the detection limit. Metabolites with a prevalence below 20% were removed.

Tensor decomposition was applied using TEMPTED[81] on log-transformed metabolite abundance, setting to 24 the number of components to identify. Temporal embeddings were used to predict treatment using hypoRF v1.0.1 (1,000 permutations, 500 trees, impurity as the 'importance' metric) [83]. Wilcoxon sum-ranked tests were used to associate individual components with treatment groups, with BH-FDR adjustment.

Univariate models between metabolites and both treatment and time were conducted as above described, using the log-10 of metabolite concentrations as the dependent variable. We tested contrasts between contiguous time points, for time effects, and contrasts between treatments, and the interaction between treatment and time, for treatment effects. We included as covariates Bristol stool scale, sex, and sample plate.

Fecal Metabolome and microbiome integration

Matching timepoints between microbiome and metabolome measurements were used for multi-view integration. We used the R package MOFA2 v1.16.0 [84], setting time as covariate (MEFISTO), and applying default options, to extract factors maximizing the variation of clr-transformed species abundances, and z-scores of metabolites. Factors were subsequently associated with time and treatment as previously described.

To link these factors with heart rate response, we computed the delta of heart rate reactivities (each reactivity defined as the delta of heart rate before and after stress challenge). The delta of pre-treatment phase and post-treatment phase was then used as the dependent variable in the analysis. As features to test, we used the 10 components per each of the three timepoints as features, so per animal we had a total of 30 features for testing.

We fitted a linear model using the z-score of the delta heart rate reactivity as dependent variable, and all 30 factor features as independent variables. We used a penalized LASSO regression approach for variable selection (glmnet R package, v4.1.8). The optimal lambda was chosen by means of a 10-fold cross-validation procedure, choosing the one that minimized the mean-squared error. Since this optimal lambda might vary depending on cross-validation random splits, we repeated this procedure 500 times and estimated per variable how many times was selected by the model, and the distribution of its estimates.

Data availability

Raw sequencing data has been submitted to SRA, under the BioProject accession PRJNA1462999..

Code availability

During the reviewing process, code has been made available to reviewers as a supplementary file. Upon acceptance, code will be made available in a public repository (GitHub/Zenodo).

Acknowledgements

We thank Rosa Argamasilla for her support conducting metabolomic measurements.

Author contributions

E.E. – Writing original draft, review and editing, conceptualization, investigation, project administration, supervision

S. A-S. – Methodology, formal analysis, writing original draft, review and editing

D.C. – Methodology, formal analysis, writing original draft, review and editing

B.T. – Methodology, formal analysis, writing original draft

A.S.B. – Methodology, investigation

G.L. – Methodology, investigation

S.K. – Methodology, investigation

A.M. – Methodology

B.K. – Methodology, investigation, project administration, review and editing

E.P. – conceptualization, project administration

M.A.B – writing original draft, review and editing, supervision

Ethics declarations

All procedures were reviewed and approved according to the principles of The Animal for Research Act of Ontario and the Canadian Council on Animal Care (CCAC) and conducted in accordance with national and international guidelines. Sample collection was performed while assuring minimal stress was experienced by the animals.

Competing interests

At the time the study was conducted, E.E., S. A-S., D.C., B.T., A-S.B., A.M., B.K., E.P., and M.A.B. were employees of dsm-Firmenich AG

Funding declaration

The study was entirely funded by dsm-firmenich AG.

References

1. Salonen, M. *et al.* Prevalence, comorbidity, and breed differences in canine anxiety in 13,700 Finnish pet dogs. *Sci Rep* **10**, 2962 (2020).

2. Barcelos, A. M., Kargas, N. & Mills, D. The Effects of Dog Behavioural Problems on Owner Well-Being: A Review of the Literature and Future Directions. *Pets* **1**, 53–69 (2024).

3. Weng, H.-Y., Morrison, J. A., Topdjian, K. & Ogata, N. Real-world data on behavioral practices for dogs in primary care veterinary hospitals in the United States (2010–2020). *Journal of the American Veterinary Medical Association* **263**, 1–7 (2025).

4. Riemer, S. Therapy and Prevention of Noise Fears in Dogs—A Review of the Current Evidence for Practitioners. *Animals* **13**, 3664 (2023).

5. Cryan, J. F. *et al.* The Microbiota-Gut-Brain Axis. *Physiol Rev* **99**, 1877–2013 (2019).

6. Kiełbik, P. & Witkowska-Piłaszewicz, O. The Relationship between Canine Behavioral Disorders and Gut Microbiome and Future Therapeutic Perspectives. *Animals* **14**, 2048 (2024).

7. Crisante, A. *et al.* A critical review of research concerning the gut microbiome in dogs and its relationship with behaviour. *Applied Animal Behaviour Science* **292**, 106755 (2025).

8. Sacoor, C., Marugg, J. D., Lima, N. R., Empadinhas, N. & Montezinho, L. Gut-Brain Axis Impact on Canine Anxiety Disorders: New Challenges for Behavioral Veterinary Medicine. *Vet Med Int* **2024**, 2856759 (2024).

9. Ephraim, E., Brockman, J. A. & Jewell, D. E. A Diet Supplemented with Polyphenols, Prebiotics and Omega-3 Fatty Acids Modulates the Intestinal Microbiota and Improves the Profile of Metabolites Linked with Anxiety in Dogs. *Biology (Basel)* **11**, 976 (2022).

10. Freijy, T. M. *et al.* Effects of a high-prebiotic diet versus probiotic supplements versus synbiotics on adult mental health: The “Gut Feelings” randomised controlled trial. *Front. Neurosci.* **16**, (2023).

11. Landsberg, G. M., Mougeot, I., Kelly, S. & Milgram, N. W. Assessment of noise-induced fear and anxiety in dogs: Modification by a novel fish hydrolysate supplemented diet. *Journal of Veterinary Behavior* **10**, 391–398 (2015).

12. Asad, A., Kirk, M., Zhu, S., Dong, X. & Gao, M. Effects of Prebiotics and Probiotics on Symptoms of Depression and Anxiety in Clinically Diagnosed Samples: Systematic Review and Meta-analysis of Randomized Controlled Trials. *Nutr Rev* **83**, e1504–e1520 (2025).

13. van de Wouw, M. *et al.* Short-chain fatty acids: microbial metabolites that alleviate stress-induced brain-gut axis alterations. *J Physiol* **596**, 4923–4944 (2018).

14. Yang, K. *et al.* Gallnut Tannic Acid Exerts Anti-stress Effects on Stress-Induced Inflammatory Response, Dysbiotic Gut Microbiota, and Alterations of Serum Metabolic Profile in Beagle Dogs. *Front Nutr* **9**, 847966 (2022).

15. Roy, A.-S. *et al.* Metabolomics provides novel understanding of Melissa officinalis mechanism of action ensuring its calming effect on dogs. *BMC Vet Res* **21**, 459 (2025).

16. Ahmed, H. *et al.* Microbiota-derived metabolites as drivers of gut-brain communication. *Gut Microbes* **14**, 2102878 (2022).

17. Rutsch, A., Kantsjö, J. B. & Ronchi, F. The Gut-Brain Axis: How Microbiota and Host Inflammasome Influence Brain Physiology and Pathology. *Front Immunol* **11**, 604179 (2020).

18. Kasarello, K., Cudnoch-Jedrzejewska, A. & Czarzasta, K. Communication of gut microbiota and brain via immune and neuroendocrine signaling. *Front Microbiol* **14**, 1118529 (2023).

19. Diether, N. E. & Willing, B. P. Microbial Fermentation of Dietary Protein: An Important Factor in Diet–Microbe–Host Interaction. *Microorganisms* **7**, 19 (2019).

20. Hyland, N. P., Cavanaugh, C. R. & Hornby, P. J. Emerging effects of tryptophan pathway metabolites and intestinal microbiota on metabolism and intestinal function. *Amino Acids* **54**, 57–70 (2022).

21. Burokas, A. *et al.* Targeting the Microbiota-Gut-Brain Axis: Prebiotics Have Anxiolytic and Antidepressant-like Effects and Reverse the Impact of Chronic Stress in Mice. *Biol Psychiatry* **82**, 472–487 (2017).

22. Zhang, R. *et al.* Impact of Enterococcus faecium Kimate-X on Reducing Stress in Dogs Through Gut Microbiota Modulation. *Vet Sci* **12**, 412 (2025).

23. Salminen, S. *et al.* The International Scientific Association of Probiotics and Prebiotics (ISAPP) consensus statement on the definition and scope of postbiotics. *Nat Rev Gastroenterol Hepatol* **18**, 649–667 (2021).

24. Kayser, E. *et al.* Effects of supplementation of live and heat-treated Bifidobacterium animalis subspecies lactis CECT 8145 on glycemic and insulinemic response, fecal microbiota, systemic biomarkers of inflammation, and white blood cell gene expression of adult dogs. *J Anim Sci* **102**, skae291 (2024).

25. Wren, J. F. *et al.* Effects of live Bacillus pumilus SG154 or a Lacticaseibacillus paracasei 327 postbiotic on apparent total tract nutrient digestibility and the immune function and fecal characteristics, metabolites, and microbiota of healthy adult dogs. *J Anim Sci* **103**, skaf231 (2025).

26. Bonel-Ayuso, D. P. *et al.* Effects of Postbiotic Administration on Canine Health: A Systematic Review and Meta-Analysis. *Microorganisms* **13**, 1572 (2025).

27. Timlin, C. L. *et al.* Effects of a Saccharomyces cerevisiae-Derived Postbiotic in Adult Labrador Retrievers Undergoing Exercise and Transport Stress. *Pets* **1**, 350–371 (2024).

28. Wilson, S. M. *et al.* Effects of a Saccharomyces cerevisiae fermentation product-supplemented diet on circulating immune cells and oxidative stress markers of dogs. *J Anim Sci* **100**, skac245 (2022).

29. Wilson, S. M. *et al.* Effects of a Saccharomyces cerevisiae fermentation product-supplemented diet on fecal characteristics, oxidative stress, and blood gene expression of adult dogs undergoing transport stress. *J Anim Sci* **101**, skac378 (2023).

30. Oba, P. M. *et al.* Effects of a Saccharomyces cerevisiae fermentation product on fecal characteristics, metabolite concentrations, and microbiota populations of dogs undergoing transport stress. *J Anim Sci* **101**, skad191 (2023).

31. Liévin-Le Moal, V. A gastrointestinal anti-infectious biotherapeutic agent: the heat-treated Lactobacillus LB. *Therap Adv Gastroenterol* **9**, 57–75 (2016).

32. Montalto, M. *et al.* Lactobacillus acidophilus protects tight junctions from aspirin damage in HT-29 cells. *Digestion* **69**, 225–228 (2004).

33. Cercamondi, C. I. *et al.* A Postbiotic Derived from Lactobacillaceae Protects Intestinal Barrier Function in a Challenge Model Using Colon Organoid Tubules. *Foods* **14**, 1173 (2025).

34. Warda, A. K. *et al.* A postbiotic consisting of heat-treated lactobacilli has a bifidogenic effect in pure culture and in human fermented faecal communities. *Appl Environ Microbiol* AEM.02459-20 (2021) doi:10.1128/AEM.02459-20.

35. Koziol, S. A. *et al.* Effects of a Lactobacillus Fermentation Product on the Fecal Characteristics, Fecal Microbial Populations, Immune Function, and Stress Markers of Adult Dogs. *J Anim Sci* **101**, skad160 (2023).

36. Warda, A. K. *et al.* Oral Administration of Heat-Treated Lactobacilli Modifies the Murine Microbiome and Reduces Citrobacter Induced Colitis. *Front Microbiol* **11**, 69 (2020).

37. Xu, X., Duarte, M. E. & Kim, S. W. Postbiotic effects of Lactobacillus fermentate on intestinal health, mucosa-associated microbiota, and growth efficiency of nursery pigs challenged with F18+Escherichia coli. *J Anim Sci* **100**, skac210 (2022).

38. Warda, A. K. *et al.* Heat-killed lactobacilli alter both microbiota composition and behaviour. *Behav Brain Res* **362**, 213–223 (2019).

39. Elhossiny, R. M., Elshahawy, H. H., Mohamed, H. M. & Abdelmageed, R. I. Assessment of probiotic strain Lactobacillus acidophilus LB supplementation as adjunctive management of attention-deficit hyperactivity disorder in children and adolescents: a randomized controlled clinical trial. *BMC Psychiatry* **23**, 823 (2023).

40. Crowell-Davis, S. L., Seibert, L. M., Sung, W., Parthasarathy, V. & Curtis, T. M. Use of clomipramine, alprazolam, and behavior modification for treatment of storm phobia in dogs. *Journal of the American Veterinary Medical Association* **222**, 744–748 (2003).

41. Jeong, Y.-K., Oh, Y.-I., Song, K.-H. & Seo, K. W. Evaluation of salivary vasopressin as an acute stress biomarker in healthy dogs with stress due to noise and environmental challenges. *BMC Vet Res* **16**, 331 (2020).

42. Lewis, S. J. & Heaton, K. W. Stool form scale as a useful guide to intestinal transit time. *Scand J Gastroenterol* **32**, 920–924 (1997).

43. Socha, H. M., Romero, M. J. & Caldwell, R. W. Oral citrulline administration enhances NO-dependent vasodilation. *The FASEB Journal* **20**, A1125–A1126 (2006).

44. Alsop, P. & Hauton, D. Oral nitrate and citrulline decrease blood pressure and increase vascular conductance in young adults: a potential therapy for heart failure. *Eur J Appl Physiol* **116**, 1651–1661 (2016).

45. Paul, P. & Holmes, W. L. Free fatty acid metabolism during stress: exercise, acute cold exposure, and anaphylactic shock. *Lipids* **8**, 142–150 (1973).

46. Townsend, L. K. *et al.* GDF15 links adipose tissue lipolysis with anxiety. *Nat Metab* **7**, 1004–1017 (2025).

47. Hsu, C.-C. *et al.* TGR5 Expression Is Associated with Changes in the Heart and Urinary Bladder of Rats with Metabolic Syndrome. *Life* **11**, (2021).

48. McEwen, B. S. Physiology and neurobiology of stress and adaptation: central role of the brain. *Physiol Rev* **87**, 873–904 (2007).

49. Fan, Z. *et al.* Dietary Strategies for Relieving Stress in Pet Dogs and Cats. *Antioxidants (Basel)* **12**, 545 (2023).

50. Dreschel, N. A. The effects of fear and anxiety on health and lifespan in pet dogs. *Applied Animal Behaviour Science* **125**, 157–162 (2010).

51. Mariotti, A. The effects of chronic stress on health: new insights into the molecular mechanisms of brain–body communication. *Future Sci OA* **1**, FSO23 (2015).

52. Carabotti, M., Scirocco, A., Maselli, M. A. & Severi, C. The gut-brain axis: interactions between enteric microbiota, central and enteric nervous systems. *Ann Gastroenterol* **28**, 203–209 (2015).

53. Ruohan, Z. *et al.* Gut microbiota as a novel target for treating anxiety and depression: from mechanisms to multimodal interventions. *Front Microbiol* **16**, 1664800 (2025).

54. Chong, H. X. *et al.* Lactobacillus plantarum DR7 alleviates stress and anxiety in adults: a randomised, double-blind, placebo-controlled study. *Beneficial Microbes* **10**, 355–374 (2019).

55. Yong, S. J., Tong, T., Chew, J. & Lim, W. L. Antidepressive Mechanisms of Probiotics and Their Therapeutic Potential. *Front. Neurosci.* **13**, (2020).

56. Motta e Motta, J. *et al.* Acute physical and mental stress resulted in an increase in fatty acids, norepinephrine, and hemodynamic changes in normal individuals: A possible pathophysiological mechanism for hypertension—Pilot study. *J Clin Hypertens (Greenwich)* **23**, 888–894 (2021).

57. Terés, S. *et al.* Oleic acid content is responsible for the reduction in blood pressure induced by olive oil. *Proceedings of the National Academy of Sciences* **105**, 13811–13816 (2008).

58. Herbel, J., Aurich, J., Gautier, C., Melchert, M. & Aurich, C. Stress Response of Beagle Dogs to Repeated Short-Distance Road Transport. *Animals (Basel)* **10**, 2114 (2020).

59. Franzini de Souza, C. C., Maccariello, C. E. M., Dias, D. P. M., Almeida, N. A. D. S. & Medeiros, M. A. de. Autonomic, endocrine and behavioural responses to thunder in laboratory and companion dogs. *Physiol Behav* **169**, 208–215 (2017).

60. Xiao, S.-D. *et al.* Multicenter, Randomized, Controlled Trial of Heat-Killed Lactobacillus acidophilus LB in Patients With Chronic Diarrhea. *Advances In Therapy* **20**, 8 (2003).

61. Xu, X., Duarte, M. E. & Kim, S. W. Postbiotic effects of *Lactobacillus* fermentate on intestinal health, mucosa-associated microbiota, and growth efficiency of nursery pigs challenged with F18+ *Escherichia coli*. *Journal of Animal Science* **100**, skac210 (2022).

62. Pilla, R. & Suchodolski, J. S. The Role of the Canine Gut Microbiome and Metabolome in Health and Gastrointestinal Disease. *Front Vet Sci* **6**, 498 (2019).

63. Essner, A. *et al.* Comparison of Polar® RS800CX heart rate monitor and electrocardiogram for measuring inter-beat intervals in healthy dogs. *Physiology & Behavior* **138**, 247–253 (2015).

64. Lensen, R. C. M. M. *et al.* Validity and reliability of cardiac measures during behavioural tests in pet dogs at home. *Applied Animal Behaviour Science* **186**, 56–63 (2017).

65. Araujo, J. A., de Rivera, C., Landsberg, G. M., Adams, P. E. & Milgram, N. W. Development and validation of a novel laboratory model of sound-induced fear and anxiety in Beagle dogs. *Journal of Veterinary Behavior* **8**, 204–212 (2013).

66. Landsberg, G. M. *et al.* Dog-appeasing pheromone collars reduce sound-induced fear and anxiety in beagle dogs: a placebo-controlled study. *Vet Rec* **177**, 260 (2015).

67. Gillespie, J. J. *et al.* PATRIC: the comprehensive bacterial bioinformatics resource with a focus on human pathogenic species. *Infect Immun* **79**, 4286–4298 (2011).

68. Coelho, L. P. *et al.* Similarity of the dog and human gut microbiomes in gene content and response to diet. *Microbiome* **6**, 72 (2018).

69. Olm, M. R., Brown, C. T., Brooks, B. & Banfield, J. F. dRep: a tool for fast and accurate genomic comparisons that enables improved genome recovery from metagenomes through de-replication. *ISME J* **11**, 2864–2868 (2017).

70. Ruscheweyh, H.-J. *et al.* Cultivation-independent genomes greatly expand taxonomic-profiling capabilities of mOTUs across various environments. *Microbiome* **10**, 212 (2022).

71. Parks, D. H., Imelfort, M., Skennerton, C. T., Hugenholtz, P. & Tyson, G. W. CheckM: assessing the quality of microbial genomes recovered from isolates, single cells, and metagenomes. *Genome Res.* **25**, 1043–1055 (2015).

72. Chaumeil, P.-A., Mussig, A. J., Hugenholtz, P. & Parks, D. H. GTDB-Tk: a toolkit to classify genomes with the Genome Taxonomy Database. *Bioinformatics* **36**, 1925–1927 (2019).

73. Wood, D. E., Lu, J. & Langmead, B. Improved metagenomic analysis with Kraken 2. *Genome Biol* **20**, 257 (2019).

74. Morgulis, A., Gertz, E. M., Schäffer, A. A. & Agarwala, R. A fast and symmetric DUST implementation to mask low-complexity DNA sequences. *J Comput Biol* **13**, 1028–1040 (2006).

75. Chen, S., Zhou, Y., Chen, Y. & Gu, J. fastp: an ultra-fast all-in-one FASTQ preprocessor. *Bioinformatics* **34**, i884–i890 (2018).

76. Lu, J., Breitwieser, F. P., Thielen, P. & Salzberg, S. L. Bracken: estimating species abundance in metagenomics data. *PeerJ Comput Sci* **3**, e104 (2017).

77. Whittaker, A. C., Ginty, A., Hughes, B. M., Steptoe, A. & Lovallo, W. R. Cardiovascular Stress Reactivity and Health: Recent Questions and Future Directions. *Psychosom Med* **83**, 756–766 (2021).

78. Pedersen, E. J., Miller, D. L., Simpson, G. L. & Ross, N. Hierarchical generalized additive models in ecology: an introduction with mgcv. *PeerJ* **7**, e6876 (2019).

79. Bretz, F., Hothorn, T. & Westfall, P. *Multiple Comparisons Using R*. (Chapman and Hall/CRC, New York, 2016). doi:10.1201/9781420010909.

80. Van den Brink, P. J. & Braak, C. J. F. T. Principal response curves: Analysis of time-dependent multivariate responses of biological community to stress. *Environmental Toxicology and Chemistry* **18**, 138–148 (1999).

81. Shi, P. *et al.* TEMPTED: time-informed dimensionality reduction for longitudinal microbiome studies. *Genome Biol* **25**, 317 (2024).

82. Shi, Z. J., Dimitrov, B., Zhao, C., Nayfach, S. & Pollard, K. S. Fast and accurate metagenotyping of the human gut microbiome with GT-Pro. *Nat Biotechnol* **40**, 507–516 (2022).

83. Hediger, S., Michel, L. & Näf, J. On the use of random forest for two-sample testing. *Computational Statistics & Data Analysis* **170**, 107435 (2022).

84. Velten, B. *et al.* Identifying temporal and spatial patterns of variation from multimodal data using MEFISTO. *Nat Methods* **19**, 179–186 (2022).

Supplementary Files

This is a list of supplementary files associated with this preprint. Click to download.

- SupplementalData.docx
- SupplementaryTablessubmission.xlsx